AD-A106 731 HONEYWELL SYSTEMS AND RESEARCH CENTER MINNEAPOLIS MN F/G 17/7
DUAL POLARIZATION FIBER OPTIC GYRO,(U)
OCT 81 J G HANSE, R B SMITH, G L MITCHELL N00173-80-C-0344
UNCLASSIFIED 81SRC75 NL

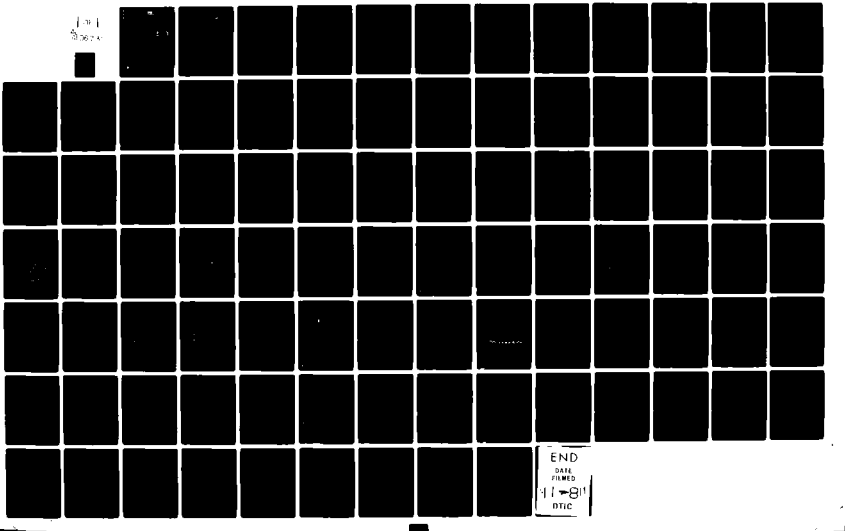

END
DATE FILMED
11-81
DTIC

81SRC75

LEVEL II

12 yu

DUAL POLARIZATION FIBER OPTIC GYRO

Final Report, Contract N00173-80-C-0344

OCTOBER 30, 1981

by

Joel G. Hanse
Robert B. Smith
Gordon L. Mitchell

Prepared for the

Naval Research Laboratory
Washington, DC 20375

Honeywell Systems and Research Center
2600 Ridgway Parkway
P.O. Box 312
Minneapolis, MN 55440

UNCLASSIFIED

SECURITY CLASSIFICATION OF THIS PAGE (WHEN DATA ENTERED)

REPORT DOCUMENTATION PAGE	READ INSTRUCTIONS BEFORE COMPLETING FORM
1. REPORT NUMBER	2. GOVT ACCESSION NUMBER: AD-A106731
3. RECIPIENT'S CATALOG NUMBER	
4. TITLE (AND SUBTITLE): DUAL POLARIZATION FIBER OPTIC GYRO.	5. TYPE OF REPORT/PERIOD COVERED: Final Report. 1 Oct 1980 — 30 Sept 1981
	6. PERFORMING ORG. REPORT NUMBER: 81SRC75
7. AUTHOR(S): Joel G. Hanse, Robert B. Smith, Gordon L. Mitchell	8. CONTRACT OR GRANT NUMBER(S): N00173-81-C-0044
9. PERFORMING ORGANIZATIONS NAME/ADDRESS: Honeywell Systems and Research Center, 2600 Ridgway Parkway, PO Box 312, Minneapolis, Minnesota 55440	10. PROGRAM ELEMENT, PROJECT, TASK AREA & WORK UNIT NUMBERS: 12 91
11. CONTROLLING OFFICE NAME/ADDRESS: Naval Research Laboratory, Washington, DC 20375	12. REPORT DATE: 30 October 1981
	13. NUMBER OF PAGES: 90
14. MONITORING AGENCY NAME/ADDRESS (IF DIFFERENT FROM CONT. OFF.)	15. SECURITY CLASSIFICATION (OF THIS REPORT): Unclassified
	15a. DECLASSIFICATION DOWNGRADING SCHEDULE

16. DISTRIBUTION STATEMENT (OF THIS REPORT)

Distribution unlimited; approved for public release.

17. DISTRIBUTION STATEMENT (OF THE ABSTRACT ENTERED IN BLOCK 20, IF DIFFERENT FROM REPORT)

18. SUPPLEMENTARY NOTES

19. KEY WORDS (CONTINUE ON REVERSE SIDE IF NECESSARY AND IDENTIFY BY BLOCK NUMBER)

Gyro	Rotation
Fiber Optics	Sensor
Interferometer	Faraday effect
Computer modeling	Scattering

20. ABSTRACT (CONTINUE ON REVERSE SIDE IF NECESSARY AND IDENTIFY BY BLOCK NUMBER)

This report presents results from a Naval Research Laboratory-sponsored investigation of dual polarization gyros. The dual polarization concept is a new fiber optic gyro configuration designed to provide independence from principal gyro bias error sources. Experimental results indicate an order of magnitude improvement in bias error performance.

Important results from a new modeling capability are also included. In addition to examination of dual polarization gyro performance, a number of fiber gyro

DD FORM 1 JAN 73 1473 EDITION OF 1 NOV 55 IS OBSOLETE

UNCLASSIFIED

SECURITY CLASSIFICATION OF THIS PAGE (WHEN DATA ENTERED)

1/02349

configurations have been examined. Results of this effort include development of an improved understanding of fiber optic depolarizers and identification of a previously unreported error term for gyros using 3 dB distributed couplers.

CONTENTS

CONTENTS (concluded)

LIST OF ILLUSTRATIONS

LIST OF ILLUSTRATIONS (concluded)

SECTION 1

INTRODUCTION AND SUMMARY

SUMMARY

This report presents results from a Naval Research Laboratory-sponsored investigation of dual polarization gyros. The dual polarization concept is a new fiber optic gyro configuration designed to provide independence from principal gyro bias error sources. Experimental results indicate an order of magnitude improvement in bias error performance.

Important results from a new modeling capability are also included. In addition to examination of dual polarization gyro performance, a number of fiber gyro configurations have been examined. Results of this effort include development of an improved understanding of fiber optic depolarizers and identification of a previously unreported error term for gyros using 3 dB distributed couplers.

GYRO ERROR TERMS

The most significant difference between rotation sensors and other sensors such as hydrophones or magnetometers is the requirement for absolute measurements. The hydrophone, for example, only needs stability for periods of time on the order of a fraction of a second. Gyros must maintain an absolute reference from hours to years, depending on the mechanization.

This absolute reference requirement is easier to meet with the Sagnac interferometer currently used for the active ring laser gyro than, for example, a Mach-Zehnder interferometer. Both geometric paths in the Sagnac are identical. Components in the Sagnac interferometer are sensitive to

environmental effects, giving rise to non-reciprocal phase shifts and, hence, a non-ideal path for light traveling in the two directions. This reduces the stability of the device, causing gyro bias errors.

It is important to note that despite the popularity of shot-noise-based error calculations, the principal problems in gyro performance have always been component-related. One of the most significant components in terms of stability is the phase modulator, which is used to achieve a $\pi/2$ offset between the two counter rotating beams. The environmental sensitivity of phase modulator components is especially important in the military gyro environment, where one normally requires instant-on performance in a rough environment without temperature compensation. Honeywell's effort has been directed at this critical phase modulator element. Evaluating a new dual polarization concept for reducing phase modulator errors is the basis of the program.

EXPERIMENTAL MEASUREMENTS

Tests reported in this document were performed with a rate table which supported the optical experiment on a small honeycomb-reinforced ferromagnetic surface. All the power and signal connections to the table were passed through slip rings, allowing for complete freedom for rotational measurements over a $\pm$120 deg/sec range. The flexibility of this test set-up allowed convenient interchanging of parts and reconfiguration of the gyro.

A dedicated computer facility was used for experimental measurements. The computer provided real time storage of data on disk files. This computer was configured to provide a display of gyro statistics during drift runs, accounting for necessary data normalization and processing. This greatly assisted the experimental set-up by providing quantitative data on gyro performance. Both analog and computer driven x-y plotters were installed as part of the measurement instrumentation package. Plots of gyro performance

contained in Section 4 of this report were generated directly by the dedicated computer facility used for the experiments. Software listings for the data processing and display functions are included in Appendix A.

In addition to the experimental efficiency provided by this computer set-up, a number of unique diagnostic capabilities were available. In one case, a laser noise term was identified by Fourier analysis of laser output and gyro detector signals. Because a large number of parameters could be recorded, it was possible to correlate variables such as temperature with other experimental data. This capability was used to provide experimental diagnostics as well as output plots.

The heart of the issue investigated in this contract effort was the feasibility of a dual polarization gyro concept. The program objective was to demonstrate that the dual polarization gyro could provide some degree of independence from bias error problems. The greatest difficulty in maintaining bias stability was expected to be the temperature dependence of the phase modulator. The experimental program described in this report had a goal of evaluating the dual polarization gyro performance in terms of these temperature problems.

Gyro operation was examined as a function of temperature. The single (conventional) polarization performance and dual polarization performance were compared. Data presented in Section 4 of this report indicate that with temperature variation, the dual polarization configuration has an order of magnitude improved bias stability.

FIBER SENSOR MODELING

A numerical solution for gyro performance was completed using a Honeywell developed interferometric model. The unique properties of this simulation are its applicability to arbitrarily large and complex systems, including dual polarization, multiple paths, and many optical components. The optical system to be modeled is described by input lines at execution time, rather than being part of program logic. This "compiler" approach allows flexibility in the modeling of complex optical systems.

A Jones vector-matrix representation was used for the optical components being analyzed. Wave amplitudes were represented by complex two-vectors for both polarizations. As the interferometric system is modeled, the total wave amplitude and absolute phase along each path are retained in a complex propagation factor. The Jones vector representation is not normalized in the conventional manner, allowing preservation of absolute amplitude along each path of the model.

In addition to the dual polarization gyro, a number of important optical components have been analyzed; results are reported in Section 3. They include a narrow-band birefringent depolarizer, birefringent fiber sections, and a simple distributed coupler gyro.

The work with the depolarizer has led to important understanding of how this component can be designed for gyro systems. Important design parameters such as the characteristics of depolarizer section length have been examined.

The effect of imperfect splicing of fibers has been considered both in the case of the dual polarization gyro and as a generic gyro component. The results of this study indicate that birefringent fibers must be carefully aligned to preserve desired gyro properties.

A fourth example which was modeled is the simple gyro configuration, which includes only a distributed coupler and sensing fiber. In this case, a significant result was the discovery of the large error term coming from distributed coupler temperature sensitivity. For small fiber optic gyros, this error can result in drift terms which amount to hundreds or thousands of degrees per hour for temperature changes on the order of 10 degrees Celsius.

SECTION 2

THEORETICAL DISCUSSION

In order to achieve fundamental performance limits in a fiber optic rate sensor, thermal mechanical and magnetic-induced errors must be removed from the device. Components, including the source, detectors, couplers and modulators (both phase and frequency), represent one class of error terms that play a major role in reducing the performance of fiber optic rate sensors. These error sources are dependent on the measurement concept and configuration.

A second more fundamental class of errors exists in the fiber itself. The non-reciprocal, scattering, and birefringent properties of the fiber are truly the practical limiting error sources in the fiber optic rate sensors. In order to achieve the projected noise performance limits, the mechanical, thermal, and magnetic errors of the fiber must be overcome.

A third problem must also be resolved to achieve the best noise-limited performance: the electronic readout technique used to detect fringe motion must be capable of detecting shifts in the range of 10^{-7} to 10^{-8} radians. This represents a significant technical challenge that must be faced in all interferometric devices.

In the following subsections, a generalized development of the Sagnac interferometer output is presented, allowing consideration of component-induced bias errors. An alternative measurement scheme involving two polarizations is discussed in detail. This dual polarization configuration has been demonstrated experimentally. Results are presented in Section 5 of this report.

FIBER OPTIC RATE SENSOR THEORY

Fiber optic rate sensing is based on the Sagnac interferometer. The classic treatment of the Sagnac effect by E.J. Post[1] shows that the phase separation between the two counter-rotating beams is proportional to the input rotation rate and is of the form

$$\Delta\phi = \frac{8\pi NA}{\lambda c}\,\Omega$$

where

N = number of turns of fiber

A = area enclosed by a single fiber loop

λ = free space wavelength of the light source

c = velocity of light in free space

Ω = input rotation rate, normal to the loop plane.

This is the classical Sagnac expression. In order to better understand the effects of errors induced in the device, it is necessary to develop a more general form of the Sagnac expression that will allow for explicit examination of the error terms.

The primary component of a fiber optic rate sensor is the closed light path that is formed into an interferometer. Light moving along the path will experience a phase change proportional to the angular rate of the path in inertial space. The sense of the phase change is determined by the direction of the light motion with respect to the angular rate. Therefore, if a light beam is split into two beams that travel in opposite directions along the light path, these two beams will experience equal and opposite phase changs. The phase changes are also proportional to the projected enclosed area whose

normal is parallel to the axis of rotation. As a result, the axis of rotation can be determined by using three independent, mutually orthogonal, closed light paths.

Consider two interferometer beams that have plane wave phase fronts in free space and in the interferometer path medium. The electric fields are described as:

$$E_1 = E_{01} \text{ Exp } i(\vec{k}_1 \cdot \vec{r} - \omega_1 t + m_1)$$

$$E_2 = E_{02} \text{ Exp } i(\vec{k}_2 \cdot \vec{r} - \omega_2 + m_2)$$

where

$\vec{k}_1$ = wave vector at frequency ω_i

m_i = arbitrary phase

E_{oi} = electric field amplitude/polarization vector

$\vec{r}$ = displacement along fiber.

The accumulated phase expression for the light beam after circulation around the path is:

$$\phi_i = \int \vec{k}_i \cdot \vec{dr} - \int_o^\tau \omega_i \, dt + m_i \quad (i = 1, 2)$$

where τ is the time required to traverse the path. For a path length $L, \tau = nL/c$, where n = the index of the medium and c = the velocity of light in space. For a system in which the observer is co-moving with the interferometer, the spatial integral is a constant and only the temporal integral is of interest. When the interferometer path is subjected to a rotation generated by velocity vector $\vec{V}$, the change in the light beam transit time can be written as[1]

$$\tau_i = \frac{1}{c^2} \int n_i (1 - \alpha) \vec{v} \cdot \vec{dr} \quad (i = 1, 2)$$

where α is a drag coefficient similar to the Fresnel-Fizeau coefficient.

The relative phase in time between the two counter-directional beams can be written as

$$\Delta\phi(t) = \phi_1(t) - \phi_2(t) = \int_0^{\tau_1'} \omega_1 dt - \int_0^{\tau_2'} \omega_2 dt + (m_1 - m_2)$$

where $\tau_i = \tau_i + \tau_i + t$. If we assume that ω_1 and ω_2 are constant, then with the refractive index and drag coefficient uniform throughout each path,

$$\Delta\phi = \frac{L}{c} (\omega_1 n_1 - \phi_2 n_2) + \frac{LV}{c^2} \left[(n_1^2 \omega_1 (1 - \alpha_1) + n_2^2 \omega_2 (1 - \alpha_2) \right] + (\omega_1 - \omega_2)t + (m_1 + m_2).$$

Consider now that the path is a circle of radius R with N turns of fiber around it. The tangential velocity V can be expressed in terms of an angular rate as $v = R\Omega$, and the path length is $L = 2\pi RN$. Using these expressions and assuming the drag coefficient to be of the form $\alpha = (1 - n^{-2})$, the phase can be written as

$$\Delta\phi = \frac{2\pi NR^2}{c^2} \Omega (\omega_1 + \omega_2) + \frac{2\pi RN}{c} (\omega_1 n_1 - \omega_2 n_2) + (\omega_1 - \omega_2)t + (m_1 - m_2).$$

points P and Q. Different choices of parameters for best distribution on the sphere are very easily explored using the computer program. Design iterations are efficient because of the flexible program structure.

This is the generalized equation for the phase difference between two counter-rotating beams in a Sagnac interferometer. This phase difference creates an interference pattern that can be observed with a photo-detector. The output of the detector is typically written as

$$I = I_0 (1 - \cos \Delta\phi).$$

Therefore, by detecting a change in the intensity of the pattern, the rotation rate of the interferometer can be determined.

For a heterodyne detection scheme, the phase equation for a single frequency can be written as

$$\Delta\phi = \frac{4\pi RL\Omega}{2c} + \frac{4\pi^2 R}{\lambda} (n_1 - n_2) + (m_1 - m_2).$$

One can clearly see that the two terms containing the index of refraction are fundamental fiber error source terms which exist in all formulations. The second is a true bias error generated by a difference in the index of refraction for the two beams. For a typical gyro, relative stability of the two indices must be better than 5×10^{-12} to reduce this term to the level of 1 deg/hr noise.

The natural sensitivity of the cosine detection function is maximized for an argument of $\pi/2$. The standard homodyne technique adjusts the $(m_1 - m_2)$ term in the previous equation to achieve this phase separation between counter-rotating beams to optimize performance. The required phase shift can be accomplished by an acousto-optic modulator which provides a different frequency for the counter-rotating beams. This causes the counter-clockwise and clockwise path to differ. An alternative way to introduce the $\tau/2$ phase shift is a nonreciprocal device such as a Faraday cell.

The Faraday cell is constructed of a material which exhibits a strong magneto-optic effect to gain the required phase shift with a small current. The Faraday cell stability, however, is a direct error term in the phase equation. This requires that overall instability of the cell be much less than the required minimum detectable rotation rate. To first order, the change of the light phase due to the Faraday effect can be written as:

$$\Theta = HLV$$

where H is an applied magnetic field, L is the length of the cell, and V is the Verdet constant. The effect in Θ can be written as:

$$\frac{\Delta\Theta}{\Theta} = \frac{\Delta L}{L} + \frac{\Delta H}{H} + \frac{\Delta V}{V}.$$

If the instrument is required to measure 10^{-5} radians and the Faraday cell is producing a $\pi/2$ phase shift, then

$$\frac{\Delta\Theta}{\Theta} \leq 5 \times 10^{-6}.$$

This sets the bounds on the stability of V, H, and L. Typical thermal coefficients on the Verdet constant are 1×10^{-4} per ^{o}C. This is nearly 2 orders of magnitude worse than required for 10^{-5} radian stability. The phase shift stability of the Faraday cell represents a major error in a homodyne detection scheme. The detector intensity for any homodyne detection scheme, ignoring fiber effects, can be written as

$$I = I_0(t)\,[1 - \cos\,(k\Omega + \Theta(t))]$$

where I_0 and Θ are varied in synchronous detection schemes. Clearly, if any unrecognized change in I_0 or Θ occurs, the net result would be a gyro bias error. Bias errors due to intensity fluctuations are generally removed by using two detectors in portions of the interference pattern which are out of phase by π. The interference patterns at the detectors can be expressed as

$$I_1 = I_o(t)\ [1 - \cos\ (k\Omega + \theta(t))]$$

$$I_2 = I_o(t)\ [1 - \cos\ (k\Omega + \theta(t) + \pi)].$$

Results can be summed and differenced to remove the laser power term. For example, let

$$Z = \frac{I_2 - I_1}{I_2 + I_1}\ .$$

The gyro output is optimized when $\theta = \pi/2$. Expanding θ to be $\theta(t) = -\pi/2 + \delta\,(t)$, where $\delta\,(t)$ is the small time dependent fluctuations of the phase modulator, the output Z becomes

$$Z \simeq \delta\,(t) + k\Omega.$$

The fluctuations of the phase modulator appear directly as a gyro bias error, causing an erroneous rate measurement. The dilemma is that there appears to be no way to remove this bias error in a standard homodyne measurement technique.

DUAL-POLARIZATION CONCEPT

The Honeywell-designed dual-polarization fiber optic gyro is a modification and expansion of the standard homodyne measurement. The basic principle is to simply operate two independent rate gyros simultaneously in the same fiber and components. Each of the gyros is a complete homodyne rate gyro; thus, the errors caused by heterodyning are avoided. If the phase modulator can be made to act oppositely for the two gyros, then it is possible to combine the outputs of the two gyros so that the modulator and its errors are removed. This is in principle the same as a so-called DILAG laser gyro. The two independent gyros can be made to coexist if their polarizations are orthogonal. The desired phase modulation will be shown to be a natural outgrowth of the orthogonal polarizations. The results of proper implementation of the concept will be:

- o Optimum $\pi/2$ phase shift for gyro sensitivity
- o 2 x increase in scale factor
- o No first-order length dependent bias errors
- o Cancellation of gyro bias errors due to the modulator.

To aid in understanding the dual-polarization performance with polarization-preserving fibers, let us define a coordinate system convention. For this discussion, we will use a coordinate system tied to the light and aligned with the orthogonal vertical and horizontal axes of the fiber. Figure 1 shows examples of linear polarization states propagating in opposite directions in two fibers. The box diagrams alongside the fibers are how the polarization state appears to the observer as he is "looking into the light" with the direction of propagation coming out of the page. If the light is circular polarized, the direction of

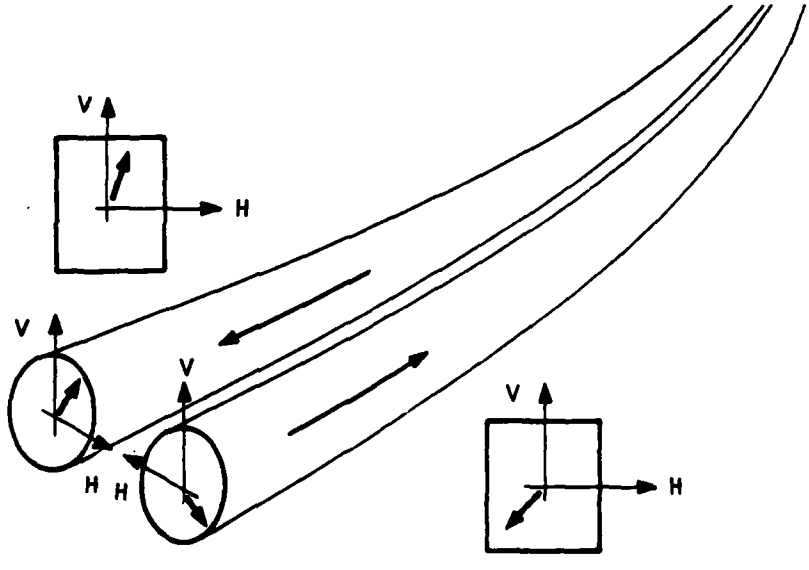

Figure 1. Fiber Polarization Convention

electric vector rotation in the fiber is represented by an arrow in the diagram with clockwise rotation indicating right circular polarization. This convention will be used in following illustrations to trace the polarization state through the dual polarization fiber gyro. In some diagrams, other information, such as the orientation of wave plate fast/slow axes or accumulated phase, will be presented with the diagrams.

Figure 2a shows a dual polarization gyro configuration using isotropic or birefringent fiber. The source polarization is aligned with the fast axis of the fiber. This beam is divided at the beam splitter, whose axis of polarization is such that the reflected beam undergoes a π phase change. The reflected beam passes through the first $\lambda/4$ plate, becomes RCP (right circular polarized), passes through the cell, and undergoes a phase retardation. The second $\lambda/4$ plate returns the RCP light to the same linear polarization as what entered the first $\lambda/4$ plate. This is a result of having the two plates rotated 90 deg with respect to each other. The linear polarized light enters the fiber aligned with the fiber fast-axis, and propagates clockwise around the loop, causing a Sagnac phase retardation. The output from the fiber is reflected at the beam splitter, accumulates another π change in phase, and strikes the detector. A perfectly isotropic fiber or one with polarization compensation can be used as well as a polarization-preserving fiber.

The other half of the light from the source beam passes through the beam splitter and through the fiber, picking up a Sagnac phase advance. In wave plate #2 it becomes RCP, and since it is passing through the Faraday cell in the opposite direction, it now experiences a phase advance. Wave plate #1 returns the RCP light to the original linear polarization, which passes through the beam splitter and combines with the counter-rotating beam to form an interference pattern whose phase difference can be expressed as

$$\Delta\phi_1 = 2\Omega + 2I.$$

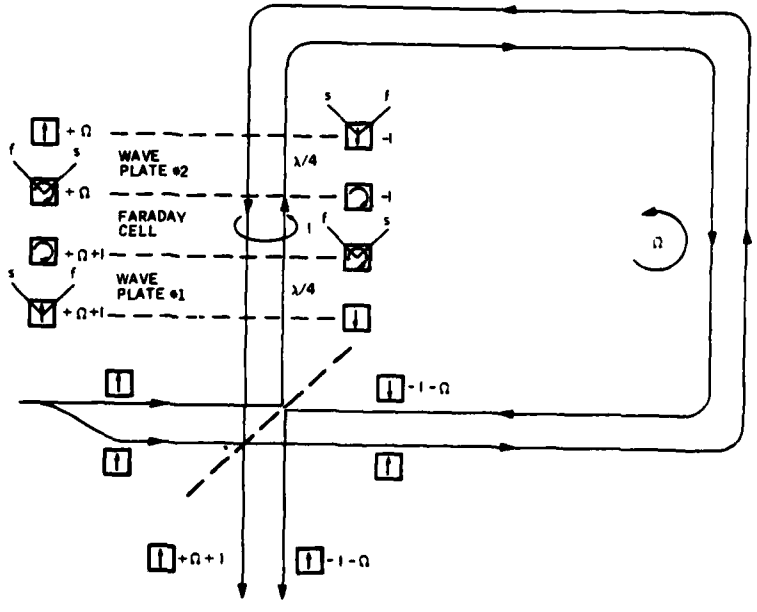

Figure 2a. Dual Polarization Gyro with S-Polarized Input Light

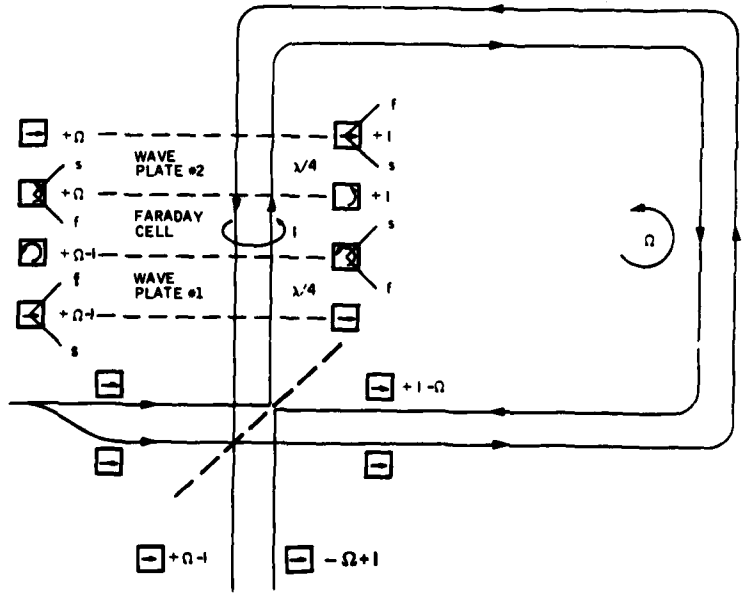

Figure 2b. Dual Polarization Gyro with P-Polarized Input Light

Now consider Figure 2b, which is the same interferometer with the polarization of the source rotated by 90 degrees. The reflected beam is not phase changed. Wave plate #1 creates LCP light which is phase advanced in the Faraday cell. Wave plate #2 returns the light to the initial polarization state; the rotating fiber coil generates a phase retardation, and the output is reflected onto the detector. The transmitted portion of the source light is phase advanced in the fiber, and is changed to LCP light by wave plate #2. Because the LCP light is passing through the cell in the opposite direction from the other beam, it will receive a phase retardation. Wave plate #1 converts the output of the Faraday cell back to the original polarization, which passes through the beam splitter to form an interference pattern with the counter-rotating beam. The phase separation of this inteferometer can be expressed as

$$\Delta\phi_2 = 2\Omega - 2I.$$

The phase output of the two polarization situations can be shown to be

$$\Delta\phi_1 = 2\Omega + \left(2I + \delta\phi_1\right)$$

$$\Delta\phi_2 = 2\Omega - \left(\delta 2I + \delta\phi_2\right)$$

where

Ω = Sagnac phase shift due to rotation

I = phase shift introduced by a Faraday cell

$\delta\phi_{1,2}$ = non-reciprocal fiber effects for the fast and slow fiber polarizations.

The intensity at the detector is therefore

$$E_1 \simeq 1 - \cos\left(2\Omega + (2I + \delta\phi_1)\right)$$

$$E_2 \simeq 1 - \cos\left(2\Omega - (2I - \delta\phi_2).\right)$$

The difference of these intensities can then be expressed as

$$\Delta E = (\phi_1 + \phi_2) + 4\Omega \left[1 + 1/2 \ I^2 + 1/4 \ (\phi_1^2 + \phi_2^2) + \frac{I}{2} (\phi_1 - \phi_2) \right].$$

Notice that, just as in the standard homodyne technique, the fiber non-reciprocal terms $\delta \phi_1 + \delta \phi_2$ appear directly as a bias error. However, the phase modulator instability enters as a scale factor error. The significance of this can be demonstrated in a simple example. Consider a homodyne measurement with a perfect fiber of length 1 km in a 0.1m diameter loop, and a perfect laser source at 0.8μ. The output phase shift would be

$$Z_1 = \frac{4\pi LR}{\lambda c} \Omega + \delta$$

where Ω is the input rate and δ is the phase modulator error. For an input rate of 10 deg/hr (4.8×10^{-5} rad/sec),

$$Z_1 = (1.27 \times 10^{-4} + \delta) \text{ rad.}$$

For the same measurement in the dual-polarization mode,

$$Z_2 = 2 \left(\frac{4\pi LR}{\lambda c} \Omega \right) \left(1 + \frac{\delta^2}{2} \right)$$

or

$$Z_2 = 2.54 \times 10^{-4} \left(1 + \delta^2/2 \right) \text{rad.}$$

Now, if an undetected modulation shift of 1×10^{-4} rad were present, the output phase shifts would be

$$Z_1 = 2.27 \times 10^{-4} \text{ rad}$$

$$Z_2 = 2.54 \times 10^{-4} + 1.27 \times 10^{-12} \text{ rad.}$$

For this 10 deg/hr input rate, the conventional homodyne gyro would read out a rate of 17.9 deg/hr, while the dual-polarization gyro would read out 10.006 deg/hr. The result clearly shows that the modulator stability in the dual-polarization scheme is no longer the major error source that it is in the standard detection schemes.

SECTION 3

SENSOR MODELING AND COMPUTER PROGRAMS

INTRODUCTION

In order to model gyro performance, Honeywell has developed a numerical interferometer simulation package. This capability has provided a unique insight into gyro component effects. The modeling results presented in this section quantify:

- o dual polarization gyro performance
- o fiber depolarizer design issues
- o the effect of birefringent fiber splices
- o significant gyro errors from distributed 3 dB couplers.

The most notable feature of this package is its applicability to arbitrarily large or complex systems with dual polarization, multiple paths, and many optical components. In addition, the optical system is described by input lines at execution time, rather than as a part of the program logic. In addition to the conventional optical elements, the input lines specify input excitation, intensity detectors and polarization analyzers, and direct the type of disposition of the detector output results.

In the research and development of fiber gyros there is a need for a capability to analyze and simulate the optical system. In order to predict performance, sensitivity, and the effect of changing parameters and imperfect components, some form of quantitative calculations would be very useful. Analytical methods quickly become intractable as the complexity of the system increases. For even the simplest fiber gyro configuration, for several optical paths, and for a few optical components, it is practically impossible

to reduce a complete analytical description to a useful form. An accurate numerical simulation would be invaluable for low cost exploration of different designs, sensitivity calculation, and performance prediction.

Honeywell has been developing a program for such a simulation, and we believe that it will be a useful tool in such work. The novel features of the program are:

1. It is applicable to arbitrarily large systems, with multiple optical paths and a large number of optical components.
2. The optical system is described by a sequence of input lines, not by the program logic. The program does not need to be changed for each optical structure to be studied.
3. Different types of "experiments" can be run, each one again determined by single input lines.
4. The program is easily expandable to include additional optical elements or experiments.

METHOD: JONES VECTOR-MATRIX REPRESENTATION

The optical system is modeled using the well-known Jones vector-matrix representation for the wave amplitude propagation along multiple optical paths. The effect of optical components on the light is represented by matrix operations. Wave amplitudes are represented by complex two-vectors for the horizontal and vertical (x and y) components, here denoted as Ax and Ay. Optical components are represented by 2 x 2 complex matrices whose diagonal elements may be viewed as propagation factors for each of the x and y wave components; the off-diagonal elements are coupling or conversion coefficients between the Ax and Ay. Standard matrices are well-known for most conventional optical components such as polarizers, isotropic or birefringent path lengths, wave plates, retarders, rotators, etc.

For modeling interferometric systems it is essential to retain, along each path, information on the total wave amplitude (power) and the absolute phase along the path. This is done by including a common complex propagation factor associated with each two-vector. Conventionally, the Jones representation assumes normalized vectors and matrices such that the total power in a path is irrelevant, and any phase factor common to both Ax and Ay is assumed to be factored out. With such an assumption it is not possible to compare (add, combine, or couple) the waves in two paths. Thus, the present method may be described as the Jones vector-matrix method, enhanced by preservation of the absolute phase and total amplitude along each path.

Beam splitters, combiners, and distributed directional couplers are also necessary optical components. These are slightly less familiar to the usual descriptions of the Jones method, but the form of the required 2 x 2 and 4 x 4 matrices is well-known.

The vector-matrix representation is ideally suited to numerical work and to computer programs. The mathematical quantities are easily calculated for any component and values of the parameters which describe it, e.g., path lengths, orientation, reflection and transmission coefficients, coupling, etc. The complexity of a system lies in the large number of its components and the multiplicity of interconnecting paths, rather than in the basic components themselves. This problem can be handled by a good computer program structure.

PROGRAM STRUCTURE

Logically there are three main parts to the program. The first part reads the input lines, one per optical component, and builds up to a description of the optical system. Pointer vectors and lists are built up which describe the operations to be carried out, in which order, and on which paths. The operations are simply the multiplication of the complex wave

amplitude of each path by the 2 x 2 matrix. This phase of the program execution may be described as a "compilation" of the optical system, to be executed later any number of times.

The compilation of the system description from the input lines is done only once. But execution for numerical output may be carried out any number of times to give the output data points vs some changing parameter such as wavelength, a rotation rate, or path length, etc.

The heart of the program is a subroutine containing a large number of small blocks of code for matrices and multiplications. A block of lines, from a few to perhaps 20, exists for each possible component. During execution, for any fixed set of parameter values, and progressing from input to output, the logical flow is to skip to each block in order, executing only those operations called for. This is done very efficiently following the pointer lists made up during the build mode. It is done repeatedly with changing parameter values during any one "experiment."

The third part of the program is another subroutine which conducts the "experiments" or simulation runs. It reads additional input lines, one or more per experiment, which describe the parameters to be varied and the values to be used, and then calculates the "data points." The detector outputs are printed or stored for each data point. Any number of different experiment runs can be carried out by successive input lines, all for the same optical system, without repeating the system description.

PROGRAM INPUT: AVAILABLE COMPONENTS AND EXPERIMENTS

The structure of the optical system and the types of numerical experiments to be simulated are controlled by a list of input lines. One type of input line defines an optical component. It specifies: a mnemonic for the component; the path or paths of which it is a part; and up to four real

parameters of the component. A different type of input line chooses the type of numerical experiment to be performed: it specifies the particular optical component(s) and parameter(s) to be varied, and defines the list or range of values to be used, as well as the disposition of the generated output.

Standard optical components include: path lengths, both isotropic and birefringent with arbitrary orientation; polarizers for linear, circular, and arbitrary elliptical polarization; Faraday cell; beam splitters and combiners, both polarizing and nonpolarizing; polarization rotators; waveplates and retarders of quarter-, half- and arbitrary length and any orientation; distributed couplers in terms of coupling coefficient, coupling length and phase mismatch; and beam splitters' combiners.

The list of available optical components includes non-standard components such as detectors of total intensity or intensity in specific polarizations, and a Stokes parameter detector, allowing the polarization state to be plotted on the Poincare sphere. These detectors, which may be positioned at any point in the optical system, do not affect beam propagation. Other non-standard components are a non-reciprocal (rotation) simulator and a "component" which specifies the excitation state of the input beam.

Additional pseudo-components are available which can duplicate or symmetrically reflect a previously input component (or set of components) to a position later in the chain. One novel input "component" with mnemonic FLOP can unfold a gyro structure. Any number of components preceding the midpoint of the fiber-coil or circular path are reflected about the midpoint, with path numbers interchanged and sense of propagation reversed. This economizes the input required, and guarantees duplication of the components and their parameters for the counterpropagation paths. The latter guarantee is important in experiments which vary a parameter of a component in the counter-propagating paths of the system.

Various types of experiments may be performed by varying: 1) any one parameter of one or several duplicated components; 2) the relative frequency of the input light beam; and 3) any two parameters in one (or duplicated) components. Parameters may be varied by specifying a list of values, or by incrementing over a range.

EXAMPLES

These examples are presented in this section following the Discussion to illustrate model capabilities:

1. Dual Polarization Gyro.
2. Narrow-band Birefringent Depolarizer.
3. Four Sections of Birefringent Fiber.
4. Basic All-Fiber Gyro, Effect of Coupler Drift.

These results are important because they represent a detailed examination of fundamental gyro error sources. The first example is central to this contract program; the others are important to recently-developed high-performance gyro configurations.

DISCUSSION

The program is just reaching fruition, so these examples only hint at the principal power of the program--the ability to do simulations of arbitrarily complicated optical systems with multiple paths and many optical components.

The limitations of the program are those imposed by the Jones method. Only monochromatic steady state can be treated at present. Consequently, the program is not usable for time-modulated systems which are becoming important for fiber gyros. For quasi-monochromatic excitation (e.g., semiconductor lasers, LEDs, etc.), it is, in fact, possible to extend the Jones formulation and the program. It is only necessary to replace the complex two-vector of the wave amplitudes by their coherency matrix. This is a trivial change in the program; the same Jones matrices are used for the optical components. It is conceivable that the program can be extended to treat the time-modulated cases, but this would probably require considerably more complexity to keep track of transit time effects. The method is also not applicable to resonator structures; those become boundary value problems.

In actual practice, an important limitation will be lack of adequate quantitative data to use with the program for realistic modeling. Many optical components are less than ideal, and too little is known about the parameters. Examples are the polarization effects in beam splitters and distributed couplers, and twist or misalignment in birefringent fibers. The modeling can be only as good as the optical parameters are well-known.

Example 1. Dual Polarization Gyro

Figure 3 shows the gyro structures as it can be modeled, both in its folded and unfolded form. All significant optical components are included. Input excitation is at +45 deg polarization, and separate detectors for x and y polarizations are used at the output. The wavelength used was $0.633.10^{-3}$ mm.

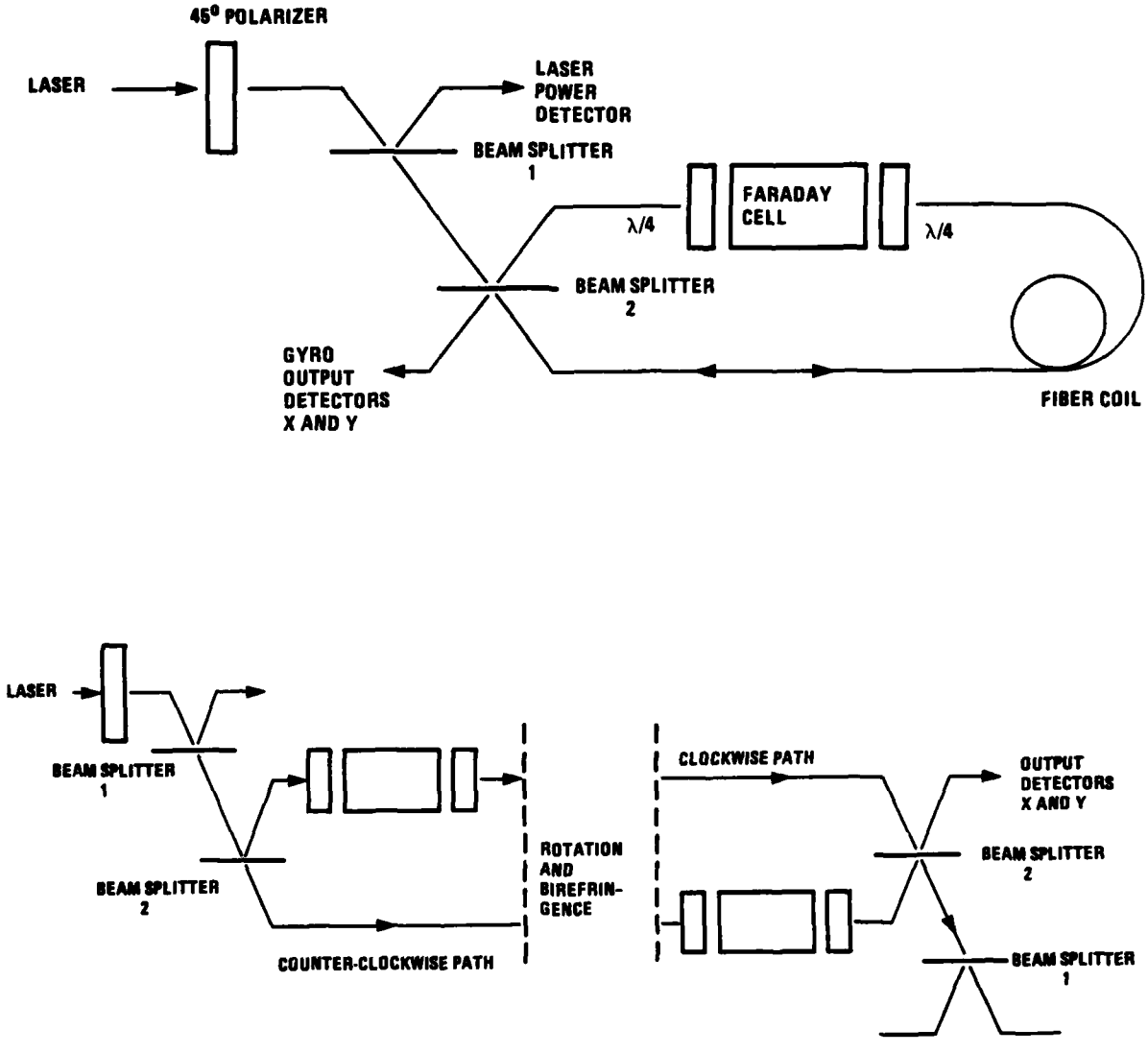

Figure 3. Dual Polarization Gyro as Modeled. Top, physical form; bottom, unfolded form simulated by computer model.

Polarization-preserving fiber with a $\Delta n = 0.15 \times 10^{-3}$ was used for the coil of 100 meters. Because a model is not yet included for a path which is both birefringent and rotation sensitive, the length was partitioned into alternating segments of birefringent fiber and nonreciprocal fiber, for a total of 50 meters of each type (with twice the retardation coefficients appropriate for a 100m length). To simulate fiber twist or misalignments, the orientation of the 3 birefringent sections could be set at $\pm$ a few degrees.

Figure 4a shows the output from the x and y polarization detectors vs rotation rate in deg/sec. Scale factor and drive for the Faraday cell were adjusted for the quadrature operating point, and the fast axis of all the birefringent fiber sections was aligned to 0 deg. The output is as expected, with the rate signal from the two detectors having opposite phase with respect to the direction of orientation. (The two polarizations are biased to complementary quadrature points.) An arbitrary scale factor was used to make this model sensitivity agree with the experimentally-observed 80 deg/sec for 2π phase shift in the detector outputs.

To simulate possible angular misalignment of the fiber, the three sections were then oriented at +5, +7, and -8 deg respectively, with the results shown in Figure 4b. Most notable is the shift from equal detector output, appearing as a drift to an equivalent +10 deg/sec rotation rate. Also, the curves are no longer symmetric--most notably, the curve for the x polarized output.

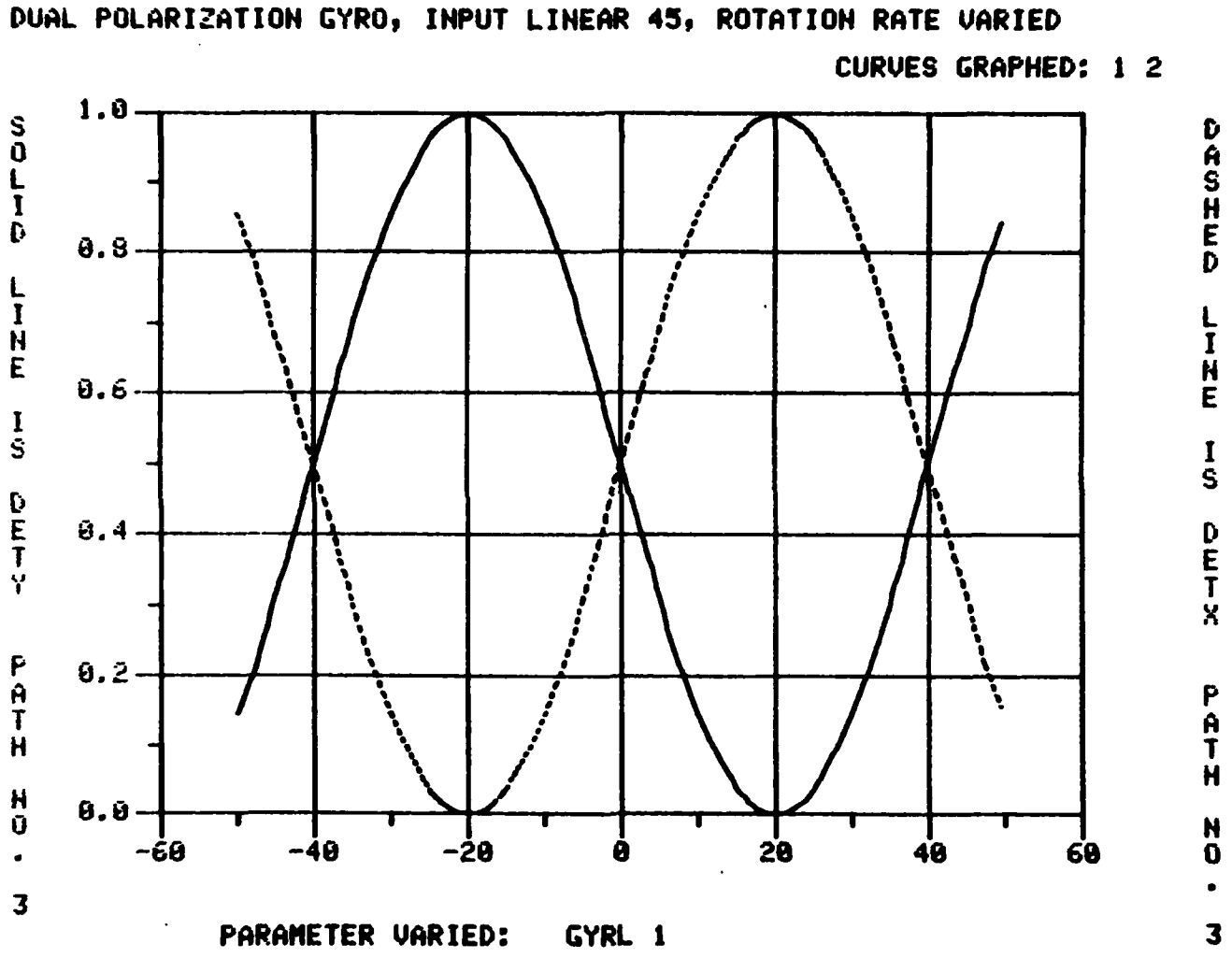

Figure 4a. Dual Polarization Gyro Operation. X and Y polarized detectors are plotted vs rotation rate in deg/sec.

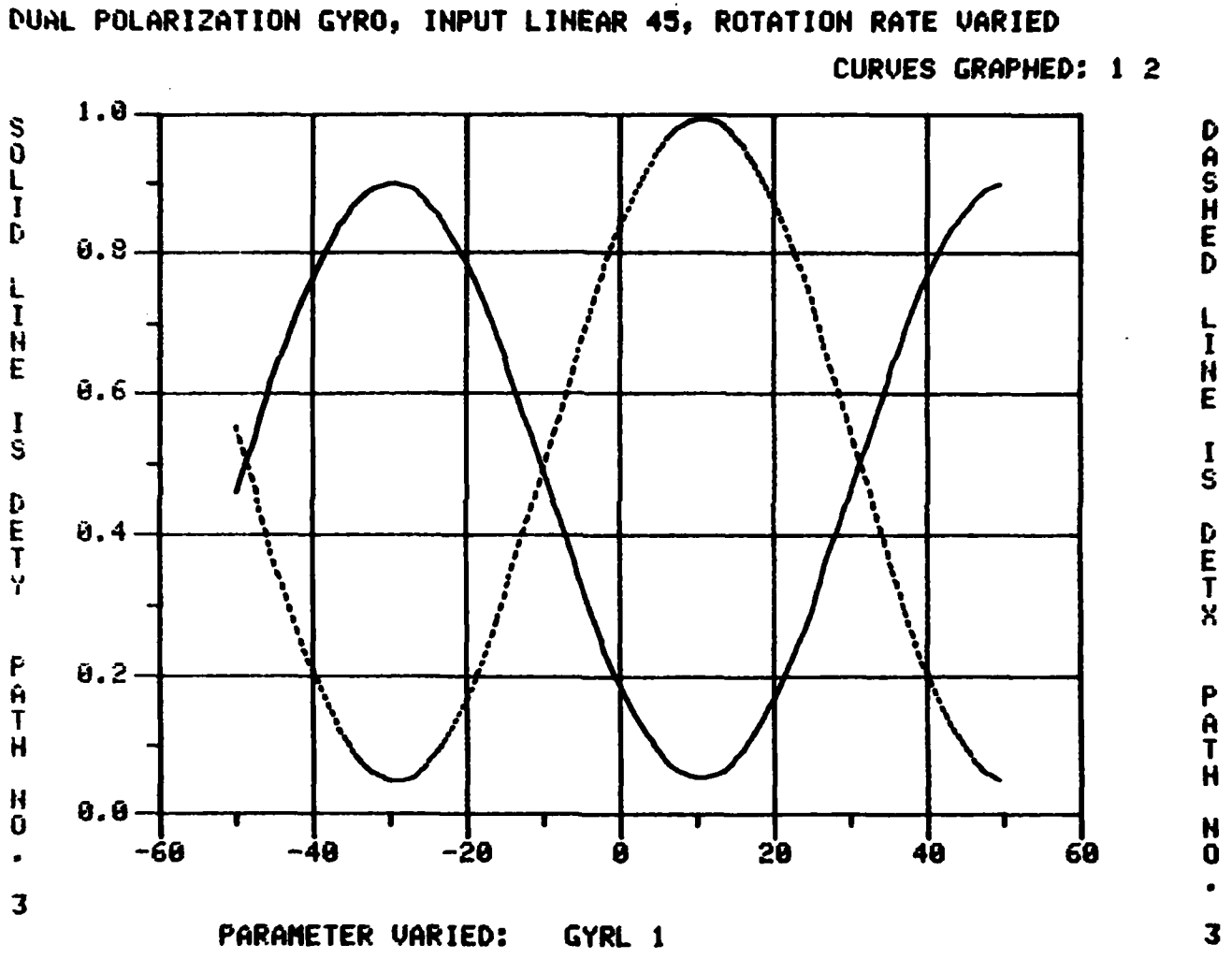

Figure 4b. Dual Polarization Gyro Operations with Fiber Splice Misalignment

A different experiment is shown in Figure 5, where the scale factor of the Faraday cell (Verdet constant) was varied over a relative range of $\pm 5 \cdot 10^{-4}$. This was intended to simulate the effects of a temperature variation of, say, ± 5 deg, assuming a temperature coefficient of 10^{-4}/deg. This demonstrates the effects of small changes, as evidenced by the expanded scales needed. The rotation rate was 0.002 deg/sec, and bias was at quadrature at the 0.15 point on the horizontal axis, resulting in 0.5 output for both detectors. The change in detector output with this "drift" in the Faraday cell was identical; the two curves have a constant separation. With respect to the sense of direction of rotation, or an apparent rotation, the sense of detector drift is opposite for the two outputs. The rotation signal, the difference between the two detectors, does not drift. This directly demonstrates the advantage of the dual polarized gyro.

Figures 6a and 6b show similar results in the presence of the birefringence misaligrment experiment previously shown in Figure 4b. We used the same change and horizontal scale for the Faraday cell scale factor as in Figure 5. Note the zero rotation rate points in Figure 4b: at about 0.19 for the x polarization, and about 0.84 for the y polarization. These points vs the drift in the bias point are shown respectively in Figures 6a and 6b. Note the expanded scales on the left for detector output. The slopes of the two curves are in the same direction, but because the two are on such different parts of their respective curves, the slopes are very different. The important point here is that the misorientation at several "joints" in the highly birefringent fiber has introducted mixing of the x and y polarized energy. The consequences are quite unpredictable.

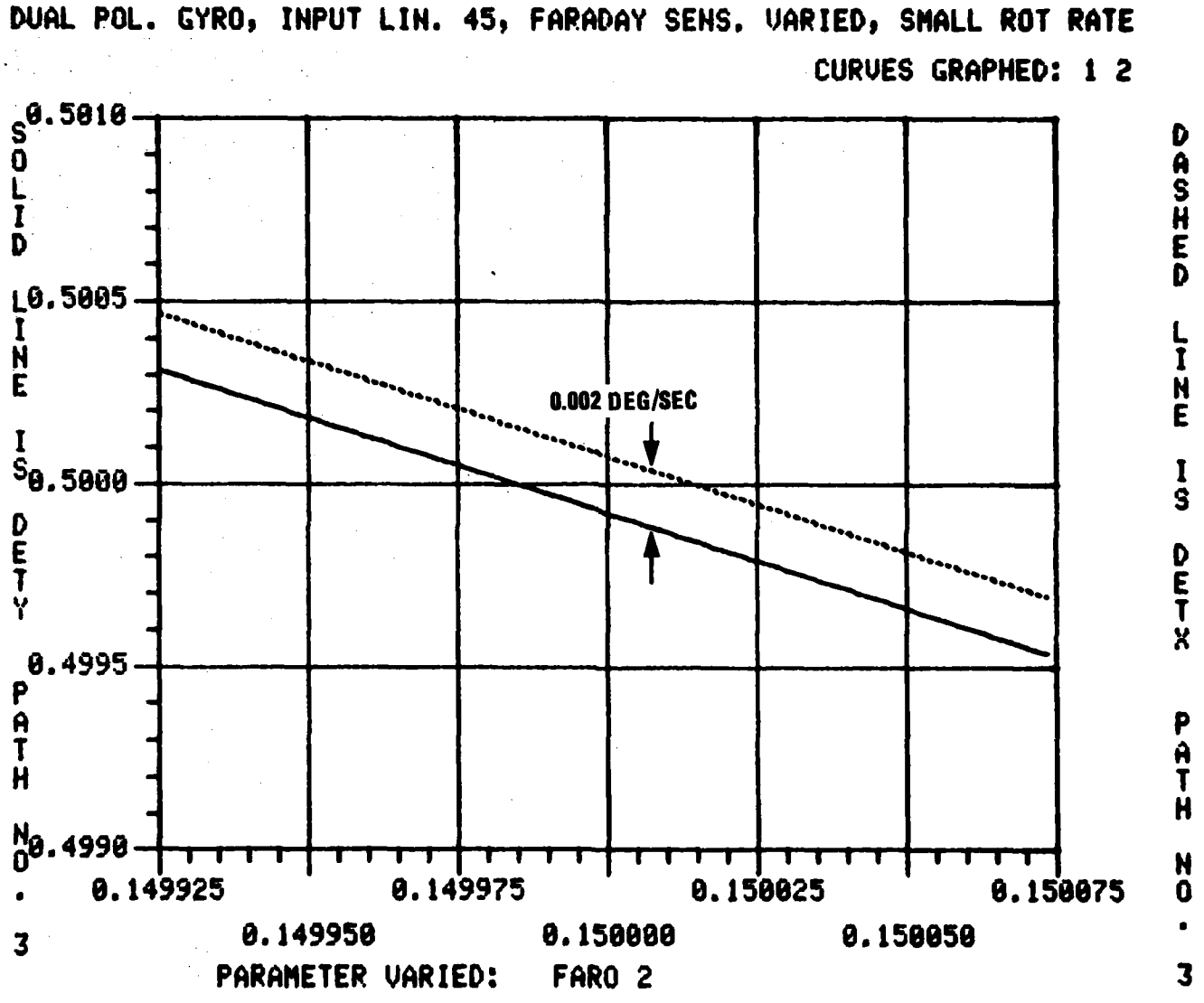

Figure 5. Dual Polarization Gyro Outputs vs Modulator Drift, Showing Bias Stability

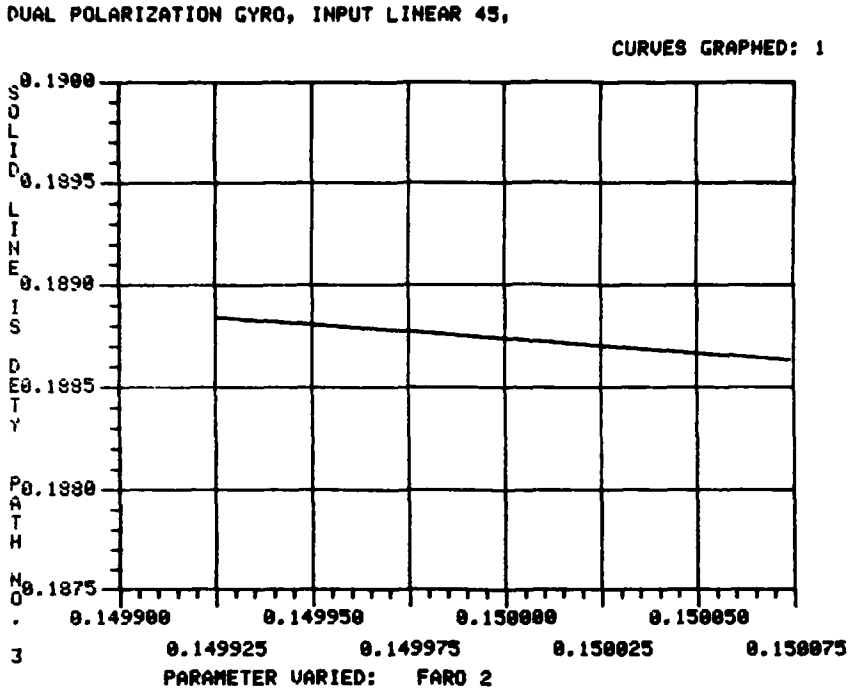

Figure 6a. Dual Polarization Output vs Faraday Cell Shift for Y Polarizations

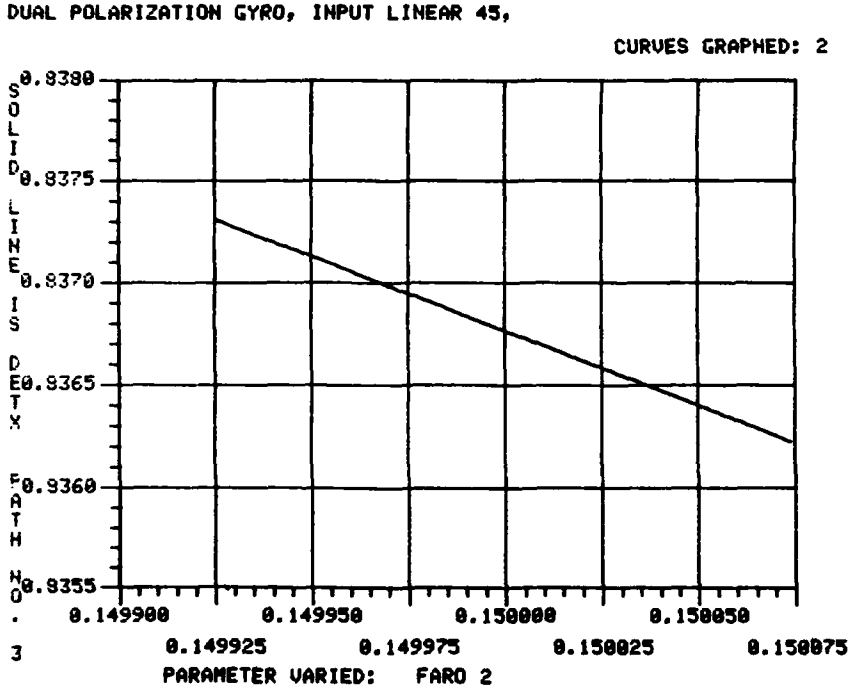

Figure 6b. Dual Polarization Output vs Faraday Cell Shift for X Polarizations

These are preliminary results and are not fully understood. The degree of misalignment is perhaps rather large, and the abrupt change is not really equivalent to fiber twist.

Example 2. Narrow-Band Birefringent Depolarizer

Rather than preserving a polarization state, it is sometimes desirable to depolarize a light source. This has meaning only for non-monochromatic light, and the bandwidth over which depolarization can be obtained is an important question. As an example, in the use of superluminescent diodes as sources for fiber gyros, a depolarizer over a 1% bandwidth is desirable.

Figure 7 shows a possible depoarizer using two lengths of quartz. For narrow-band performance, the pieces need to be rather long, depending on the degree of birefringence. One example given in the literature states that the longer piece should be twice as long as the short piece.[2] It can be shown that this is a poor choice; rather, the two lengths should have a ratio not near the ratio of small integers. The total length, in number of retardation wavelengths at center band, should be many times the inverse relative bandwidth.

The Poincare sphere is very useful to exhibit the spreading of the polarization states by a depolarizer.[3] In a good depolarizer, as the frequency of the light is varied within the bandwidth, the state of polarization is redistributed widely and uniformly over the surface of the sphere. The lower part of Figure 7 shows the points on the sphere which were obtained using the computer program. (This model requires a simple list of about 10 input lines.) The relative frequency was varied over the range of 0.995 to 1.005 using 100 points. That is, the total spectral range displayed is one percent, and the individual points shown are spaced at 10^{-4}. Good distribution over the sphere is evident, although there is a somewhat greater number of points (loops) near the $\pm$45 deg linear polarized

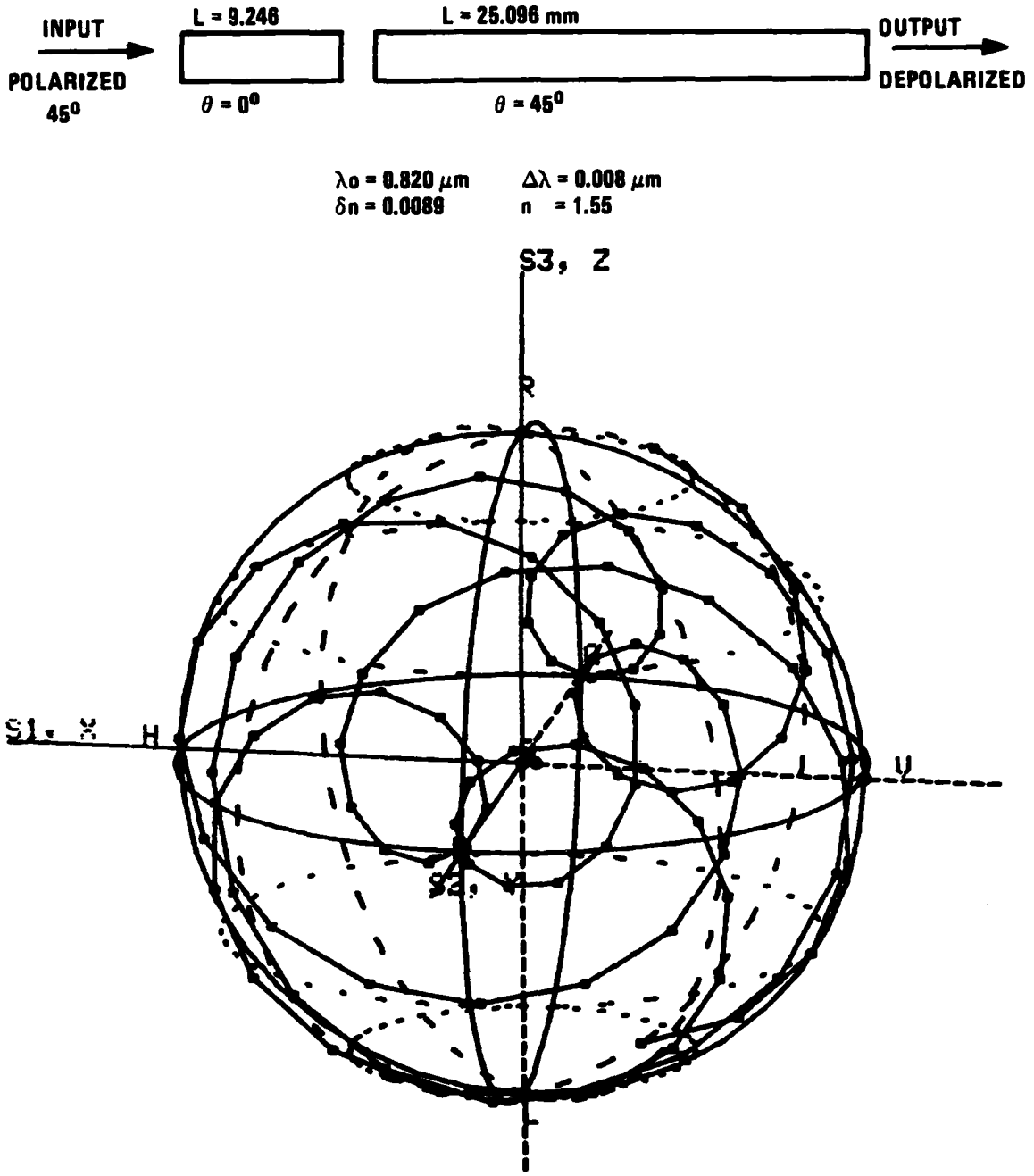

Figure 7. Narrow-Band Two-State Birefringent Depolarizer. Locus of polarization states on Poincare sphere over a 1% spectral range.

points P and Q. Different choices of parameters for best distribution on the sphere are very easily explored using the computer program. Design iterations are efficient because of the flexible program structure.

Example 3. Four Sections of Birefringent Fiber

The results from a simple example of birefringent fiber sections misoriented in angle at their junctions are shown in Figures 8 and 9. Four sections of fiber with a linear birefringence of $\delta n = 2 \cdot 10^{-7}$ were used (beat length of 2.5 meter at $\lambda = 0.5 \cdot 10^{-3}$mm). Lengths were 9.5, 9.09, 9.72, and 9.45 meters; and the orientations (fast axis) were all nominally 45 deg, but actually misoriented to 41, 47, 50, and 45 degs respectively. Input light polarized at 45 deg. is nominally aligned with the fast axis of the fiber, and should emerge as 45 deg polarized light. But the fiber misorientation will result in deviations from pure 45 deg. polarization, as is clearly shown in the two figures where the relative frequency was varied over the range 0.95 (0.001).05.

Figure 8 shows the output from x and y polarized detectors. The sum of the two is constant (energy conservation); and where the two are equal, the azimuth of the polarization is 45 deg, though there will generally be some ellipticity. More clearly displaying the departure from the +45 deg. polarization state is the locus shown on the Poincare sphere in Figure 9. The locus spirals around the point P, or Stokes parameter axis S2. Over a wider frequency band the spiral path repeats periodically. Projecting this locus onto the S1 axis from H to V gives the resolution into x and y polarization shown in the previous figure.

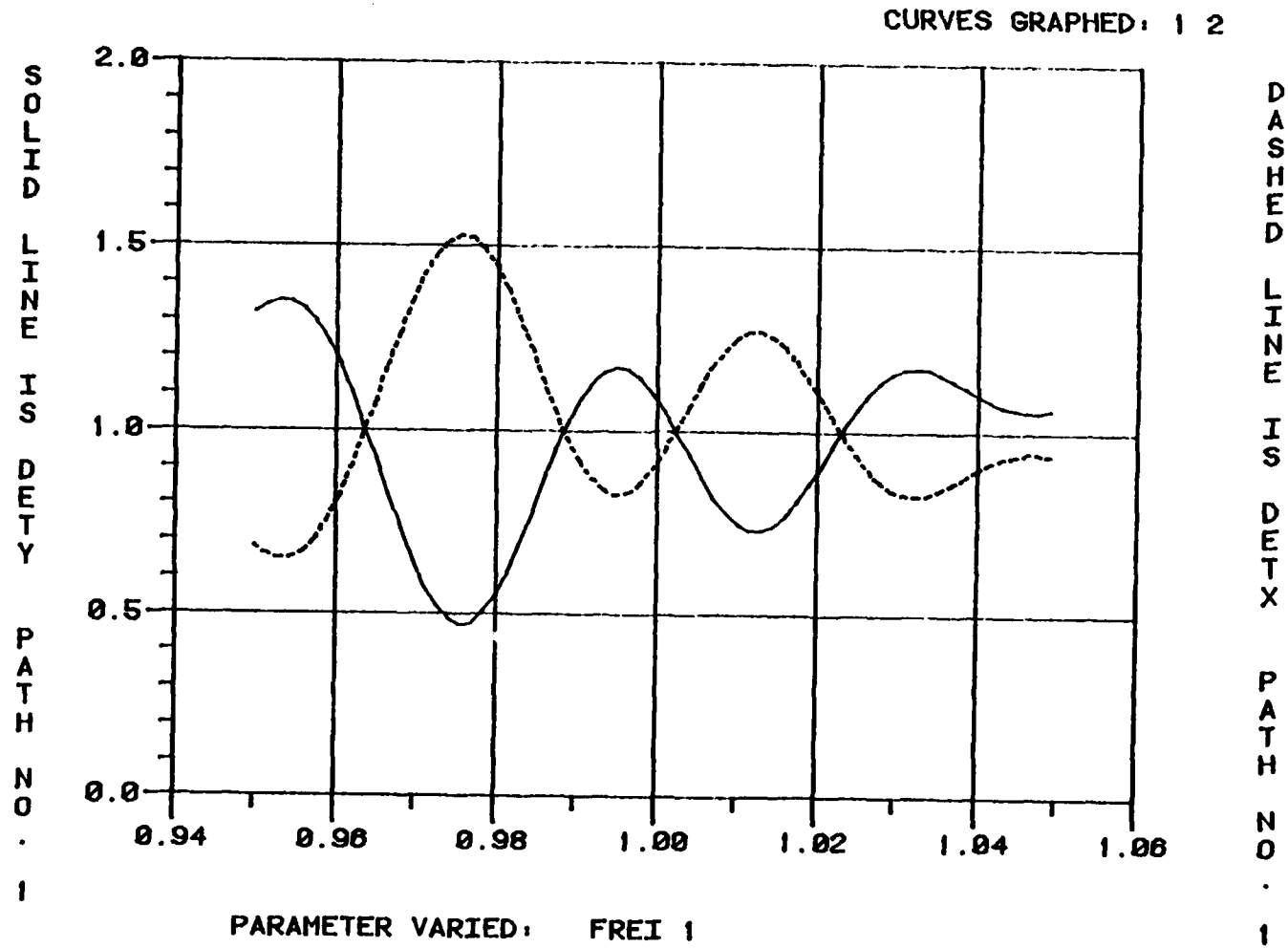

Figure 8. Output from X and Y Polarization Detectors vs Relative Frequency

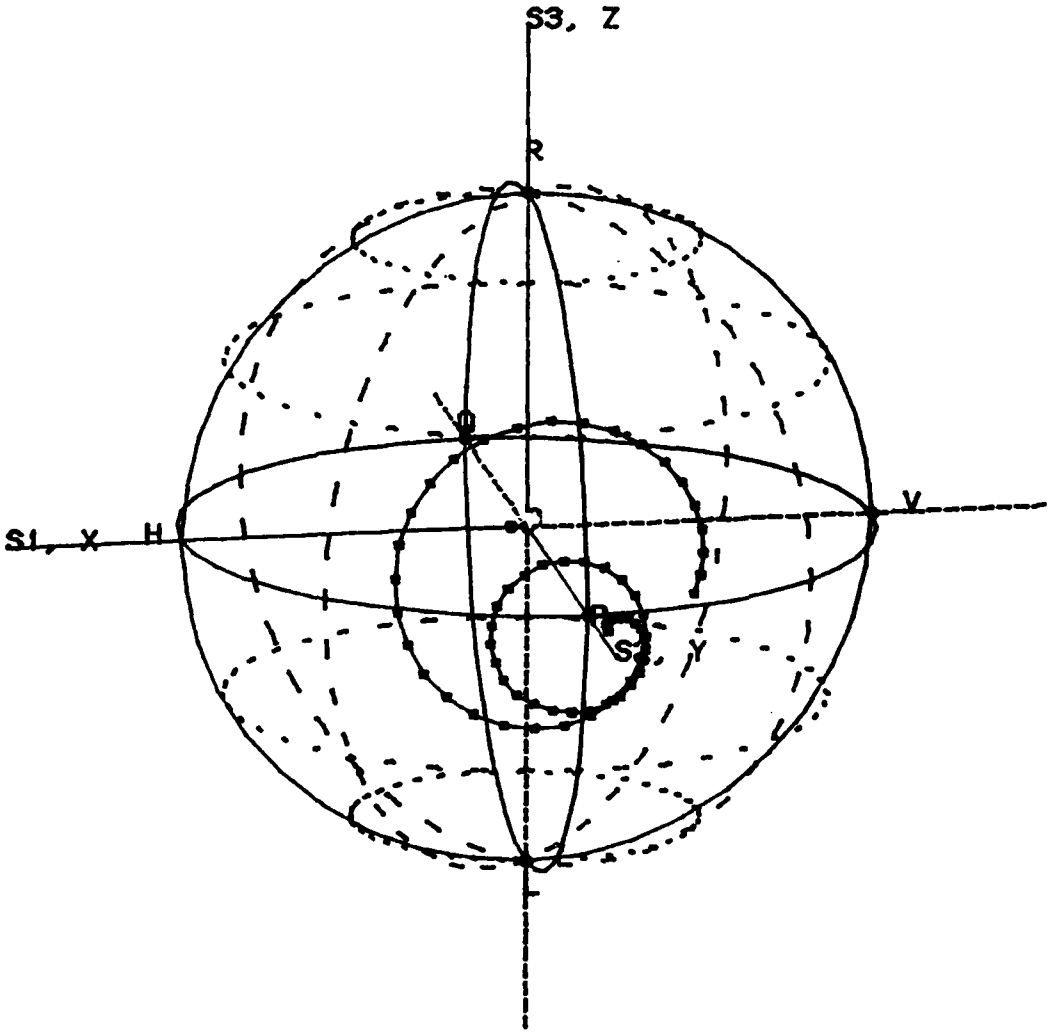

Figure 9. Output from Four Sections of Misaligned Birefringent Fiber vs. Relative Frequency. Locus of Polarization State on Poincare Sphere

Example 4. Temperature-Induced Bias Errors in Gyros Using Distributed Couplers

The basic all-fiber gyro consists of a distributed 3 dB fiber coupler used for a beam splitter/combiner plus the rotation sensing fiber coil. This may be modeled quite simply, with a single non-reciprocal phase retarder in the path to establish the quadrature operating point. Two unfolded paths are used for the clockwise and counterclockwise beams respectively, with a single detector for the output of each path, giving complementary rotation signals. Only a single polarization is used.

An experiment of interest is how the output signal might drift with, say, temperature changes in the distributed coupler. It is not obvious whether the drift would be equivalent to, or be interpreted as, a rotation signal, but this is easily modeled. Figure 10 shows the results of varying the coupling coefficient of the distributed coupler (this is equivalent to varying the effective coupler length or the frequency of the light). The consequence is that the light is not equally divided between the two paths. It is the coupling coefficient which is varied here, not the power division ratio. Because of the nature of the distributed coupler, a phase shift also accompanies the power division change; this is a phase change that appears as a gyro bias error.

With the choices of wavelength and coupler length used, equal power division required a coefficient of 0.25×10^{-5} per unit length. This point is shown circled in Figure 10. At quadrature and zero rate, the detectors for the two outputs are equal. Along the horizontal axis, the coupling coefficient is varied over a wide range. The detector outputs vary in a manner indistinguishable from a rotation rate. To first order, very near the $\pi/2$ point, the effect vanishes; but the second order effect, for changes of even one percent in the coefficient, still can be large compared to the rotation rates to be measured.

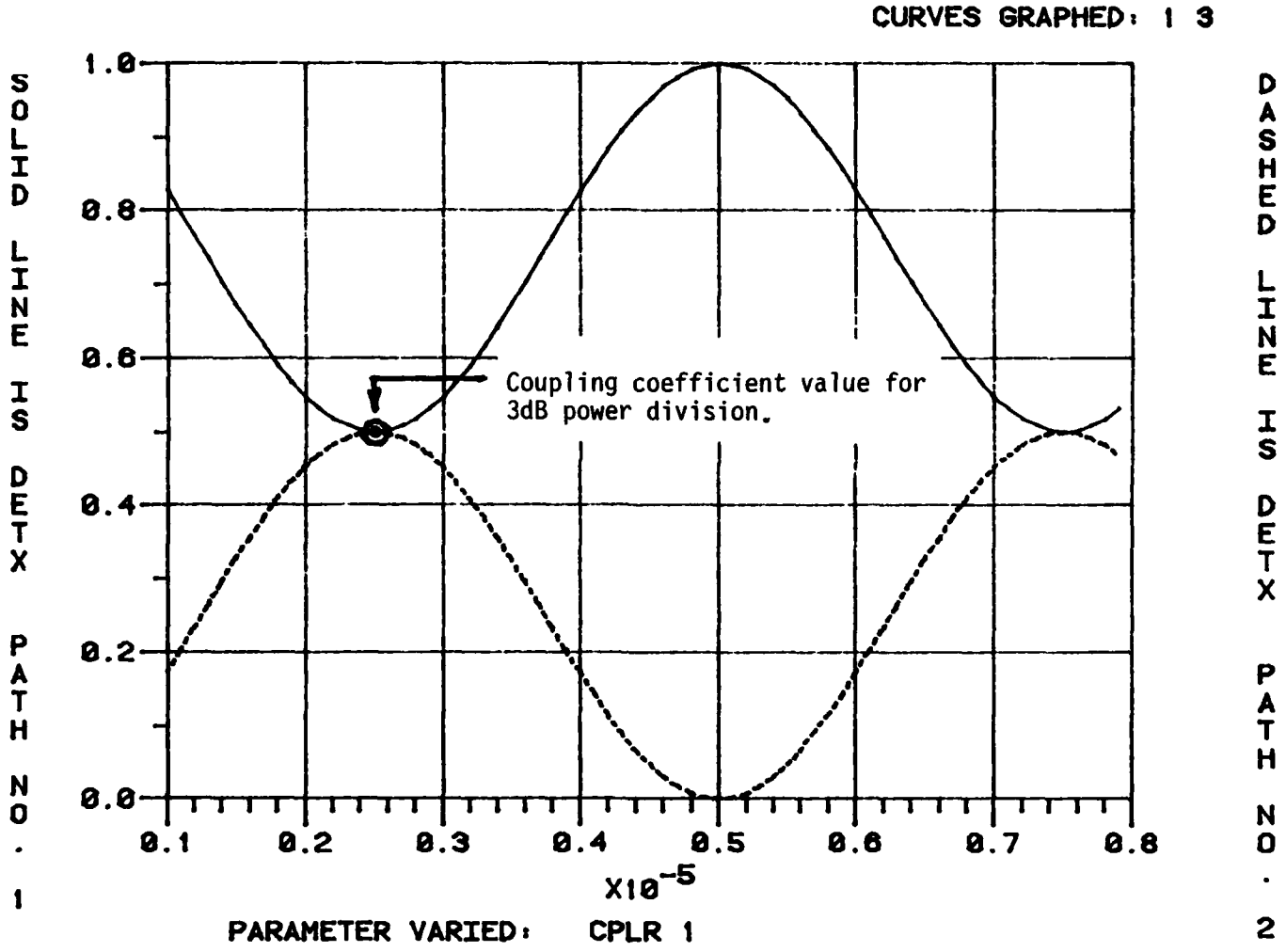

Figure 10. Output from Clockwise and Counterclockwise Beams in Basic Fiber Gyro Operating at Quadrature. Coupling Coefficient of Distributed Coupler Beam Splitter/Combiner Is Varied.

For typical gyro parameters and a few degrees temperature change, this error term amounts to hundreds of degrees per hour. The magnitude of this effect has not generally been recognized. It may present a fundamental limit to fiber optic gyro performance.

SECTION 4

EXPERIMENTAL RESULTS

A significant portion of the objective of this contract was to determine the operating parameters of the dual polarization gyro. The most fundamental part of this is the definition of concept feasibility. This includes demonstration of the experiment with measurements to evaluate performance of the gyro at quadrature, and especially to observe the effect of rotation and Faraday cell bias on the two polarizations.

The most important result, described later in this section, was demonstration of dual polarization gyro performance with a changing phase bias element environment. Gyro bias is shown to be an order of magnitude more stable in the dual polarization configuration than with only one polarization operating.

GYRO COMPONENTS

The experimental set-up used is shown in Figure 11. Here optical components are arranged on a plate which has been mounted on a rate table. Fiber is wound around the periphery of the plate. In this experiment approximately 150 meters of fiber are used on a 0.9 meter diameter circle. A Tropel 100 helium-neon light source is used for the initial experiment. This laser produced noise due to light feedback from the experiment. In later arrangements a Faraday cell isolator was used to reduce the returning light, thereby reducing oscillations in the laser. Laser output power is sampled, as shown, by detector 3. This power measurement and others at various places on the table are connected to a dedicated computer facility used to record data, analyze performance, and plot gyro characteristics.

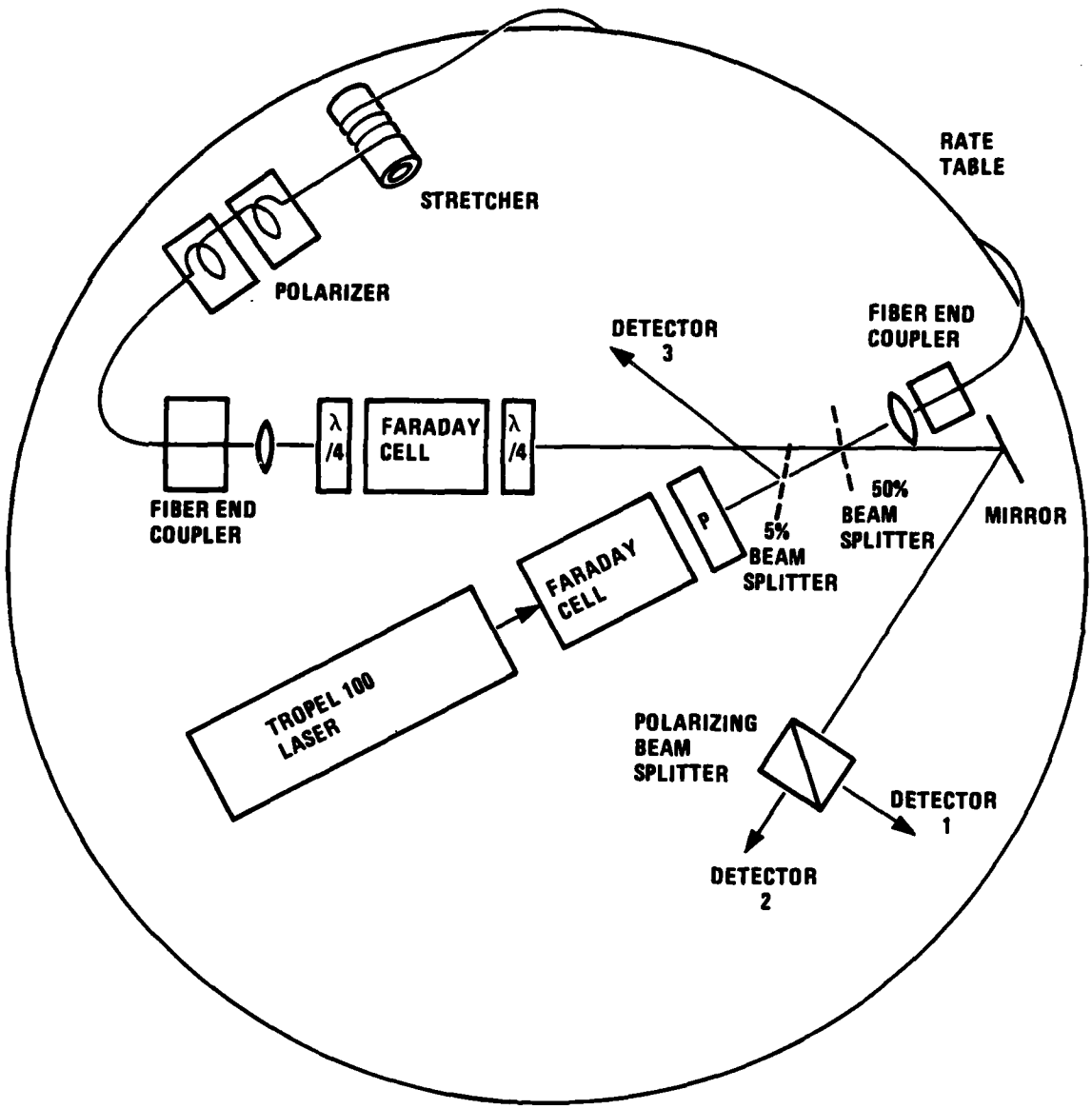

Figure 11. Gyro Component Arrangement or Rate Table

The 50% beamsplitter which allows coupling light to both fiber ends is made from a quartz substrate and designed to work at near normal incidence, minimizing polarization-dependent effects. A second Faraday cell with associated quarter wave plates provides the non-reciprocal element needed for dual polarization gyro biasing. Quarter wave plates on either end of this Faraday cell are aligned with a 90^{o} difference with respect to each other.

Fiber end couplers consist of a low strain microscope objective and a 3-axis differential screw translation stage. One end of the fiber passes through a polarizer[4] and, for some configurations, it has a fiber stretcher for decorrelation of fiber scattering. Because the gyro runs two polarizations simultaneously, it is necessary to have detectors arranged for each; in this case, a polarizing beam splitter is used for signal separation at the output of the gyro.

The optical components on the rate table are connected through a slip ring assembly to a dedicated computer data retrieval system. This is centered around a Fluke model 1720 A instrument controller. This system includes an analog scanner which feeds a remotely controlled 6-1/2 digit voltmeter. Data is stored in the 1720 A memory, processed, and then stored on disk file. This portion of the system is illustrated in Figure 12.

A function generator and power amplifier are also connected to the slip ring assembly. They are used for experiments requiring PZT stretchers for decorrelation of Rayleigh scattering within the fiber.

SOFTWARE

The experiments run on the fiber optic gyro program used a Fluke 1720A data controller as the main data storage and analysis device. The 1720A is a 16 bit micro computer with a floppy disc storage media. The language used is

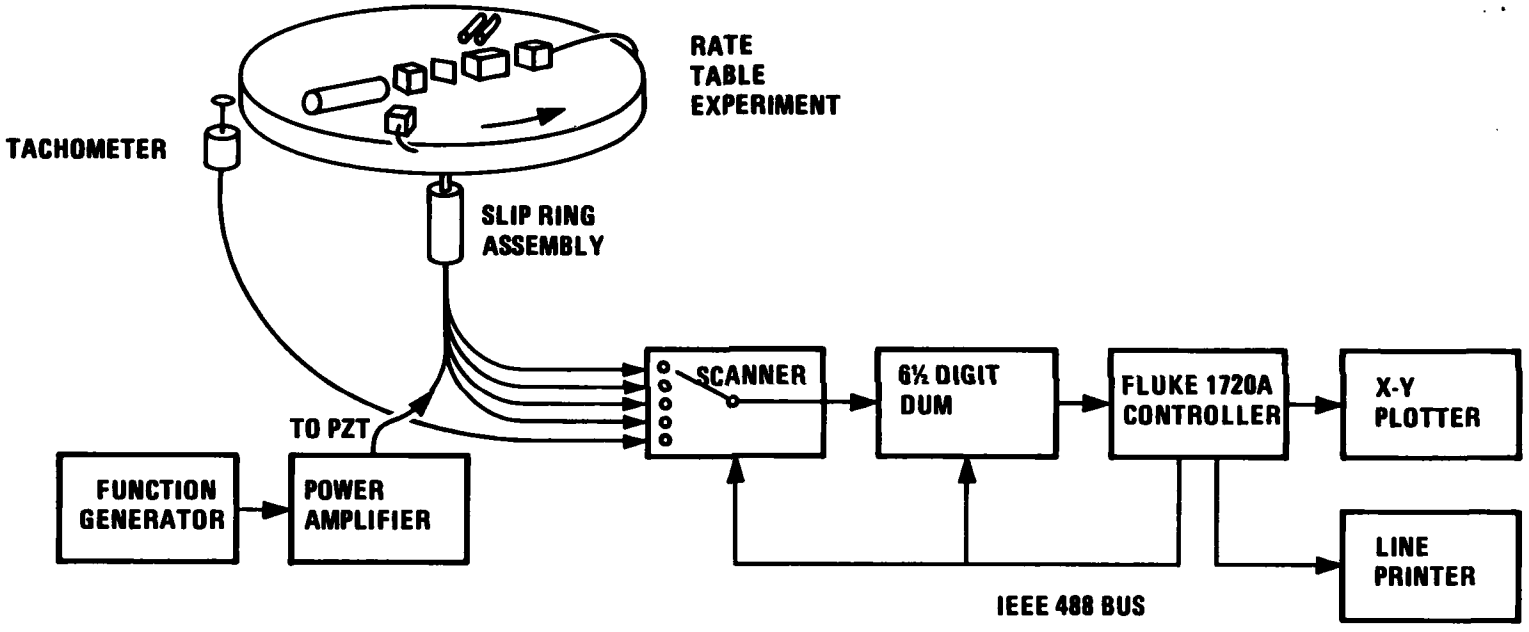

Figure 12. Computer-Controlled Data Collection Equipment Hook-Up

enhanced Basic. All the special drivers to control the IEEE-488 data bus which connects the outside world to the CPU are resident in the Basic operating system.

The routines used to acquire, analyze and plot the experimental data were generated by Honeywell personnel. They make full use of the 1720A's capabilities as a simple dedicated experiment controller. The programs developed are DATRUN, a data acquisition routine; DPDEV, a data acquisition and real time analysis routine; DPSTAT, a statistical analysis routine; RATMAX, a rate data pre-processing routine; and HPLOT1, a data plotting routine. Details of these software packages are contained in Appendix A.

STATISTICS AND NORMALIZATION

The output of the dual polarization gyro detectors is a voltage. The functional form of this voltage is

$$V = V^o \sin K\Omega$$

where V^o is the intensity scale factor of the output and K is the rate scale factor. K is determined uniquely by the gyro parameters and is written as

$$K = \frac{4\ LR}{\lambda c}$$

where

L = fiber length = 150m

R = loop radius = .5m

λ = optical wavelength = $.633 \times 10^{-6}$m

c = speed of light = 3×10^8 m/sec.

For this gyro, $K\Omega$ = 5 radians/rad/sec.

The intensity scale factor V^o is determined by the laser power, fiber losses, fiber coupling coefficients, general set-up, and detector scale

factor. Because of the flexibility of our experimental set-up, this Vo has had the opportunity to vary. We made no real effort to fix this value throughout our tests. We only required that it was known for the configuration being tested. The value is easily determined experimentally by a rate variation experiment where the input rate is varied such that $K\Omega$ traverses an angle greater than 2π.

For the most part, Vo = 6 volts. Some data plots have a different Vo. In those cases, Vo is recorded on the plot.

In order to determine the gyro performance in real units, i.e., deg/hr, we would normally have to invert the equation $V = Vo \sin K\Omega$ to the form

$$\Omega = \frac{1}{K} \sin^{-1}\left(\frac{V}{Vo}\right)$$

Practically speaking, this is a difficult process to implement and is not really necessary for experiments. The sensitivity of the gyro can be described in terms of the standard deviation of the rate data. This can be written in terms of J_V as

$$\sigma_\Omega = \sqrt{\frac{1}{Vo^2 K^2 \cos^2 K\Omega}}\ \sigma_V$$

or, for a zero rate drift run,

$$\sigma_\Omega = \frac{\sigma_V}{KVo} \quad .$$

Because the dual polarization can operate at quadrature at zero rate, the voltage-to-rate conversion can be approximated at low rates by

$$V \tilde{=} VoK\Omega.$$

Therefore, the zero rate drift test results, which are presented in volts, can be easily converted into true rate values.

EXPERIMENTAL RESULTS

The dual polarization gyro principle described in Section 2 of this report was verified and is illustrated in the following figures. Using the breadboard set-up of Figure 11, we were able to change optical components and vary experimental conditions to optimize the gyro operation. Figure 13 illustrates a dual polarization gyro output showing the horizontal and vertical detector signals. This plot shows several of the unique features of dual polarization configurations.

At zero-rate the two outputs are observed to be at the quadrature point ($\pi/2$), and of opposite slope. This situation is obtained with the gyro aligned for maximum output. These two polarization outputs have been combined algebraically in Figure 14. Comparing Figures 13 and 14, one can note that the scale factor for the gyro has been increased by a factor of two and the noise decreased. The nature of the noise is obvious from re-examining Figure 13, in which the correlated peaks can be seen.

NOISE REDUCTION TECHNIQUES

In order to decrease the noise in the gyro output, we analyzed noise sources. The most fruitful portion of this centered on laser-generated noise. Figure 15 illustrates a typical gyro output power spectral density for a drift run (constant rate input). Here the noise peak at approximately 4.0 KHz is similar to the power spectral density noise peak for the laser output. The laser output power spectral density is shown in Figure 16. This information led us to conclude that some form of laser isolation was required.

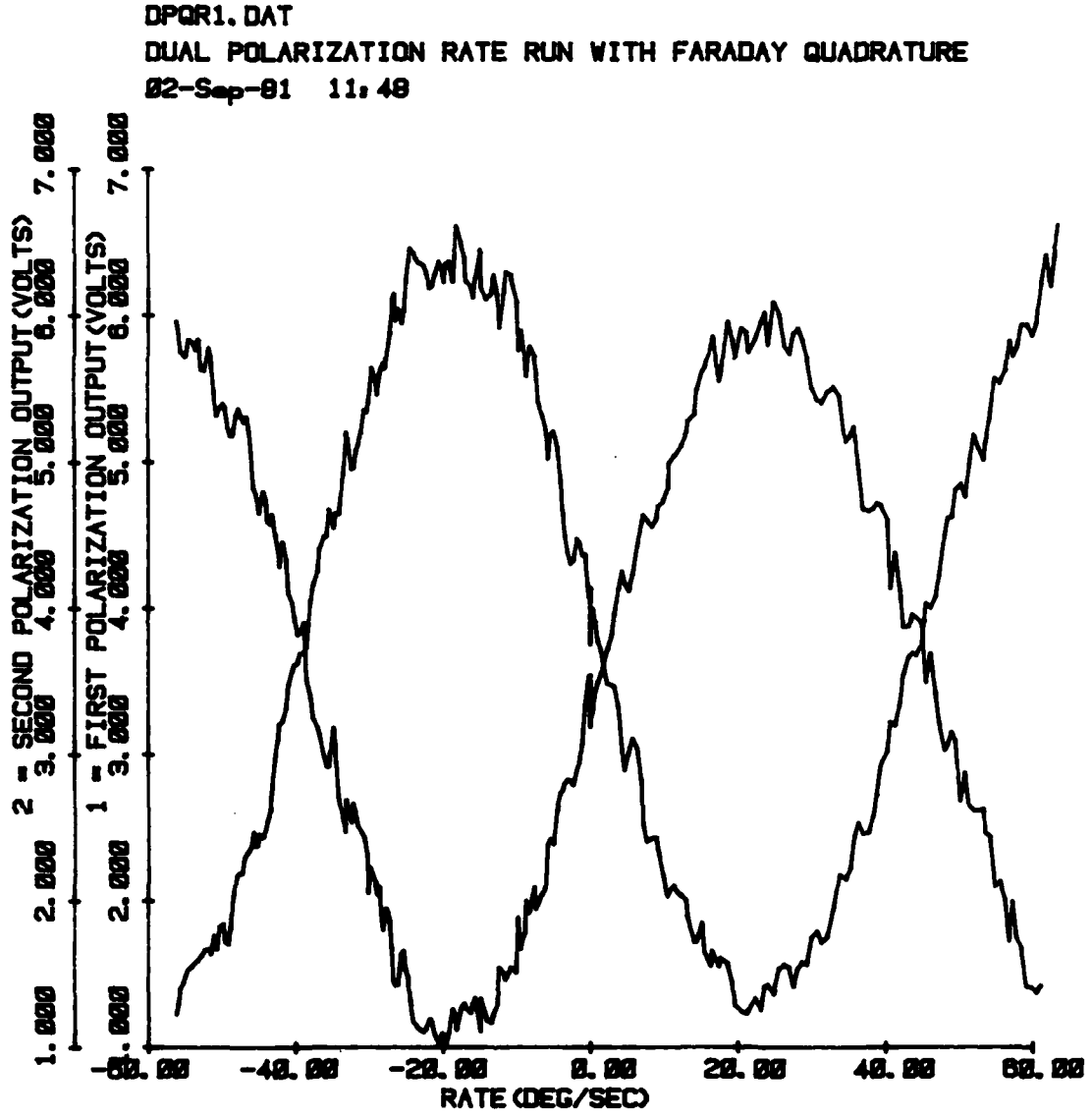

Figure 13. Gyro Output vs. Rotation Rate for Horizontal and Vertical Gyro Polarizations

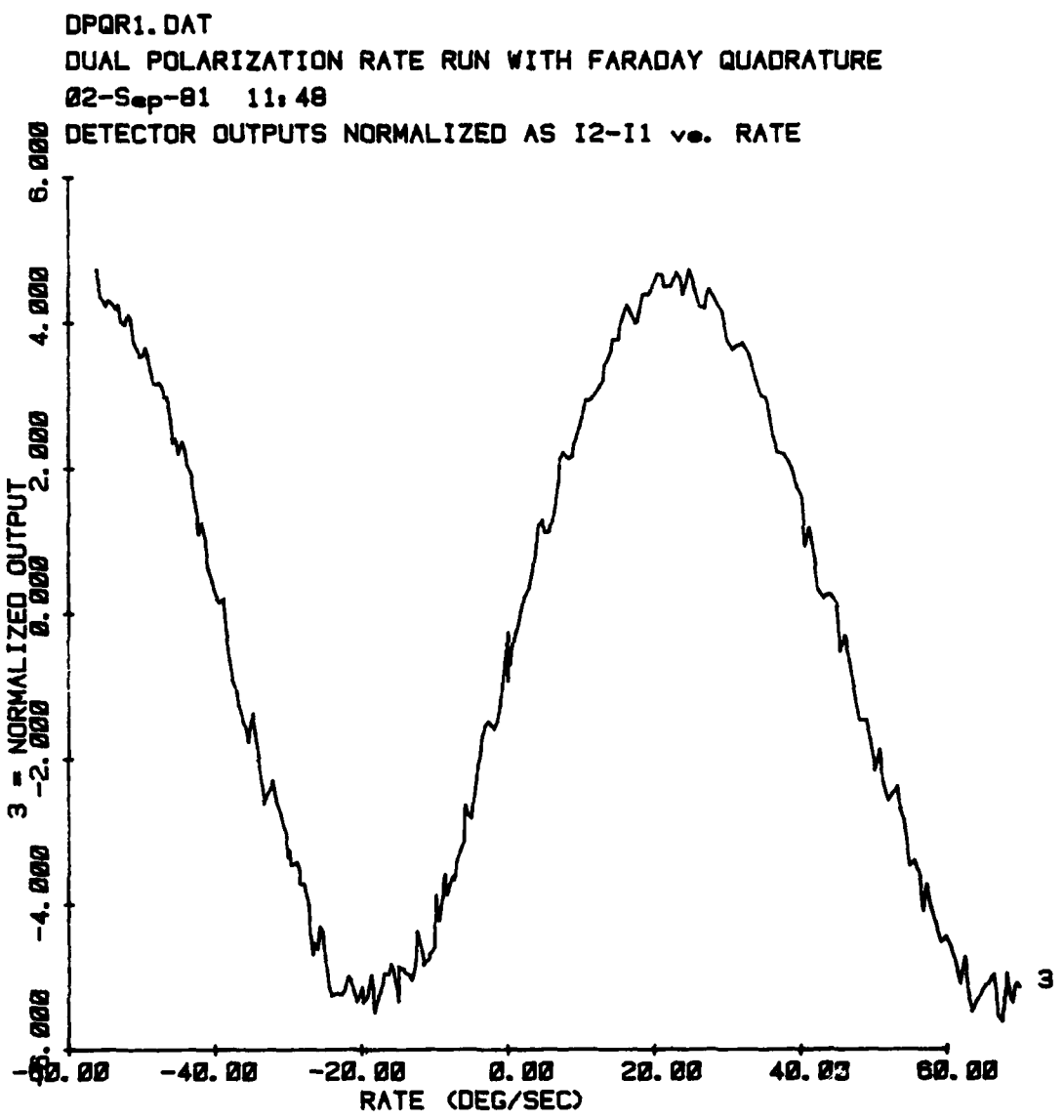

Figure 14. The Combination of Two Polarization Outputs

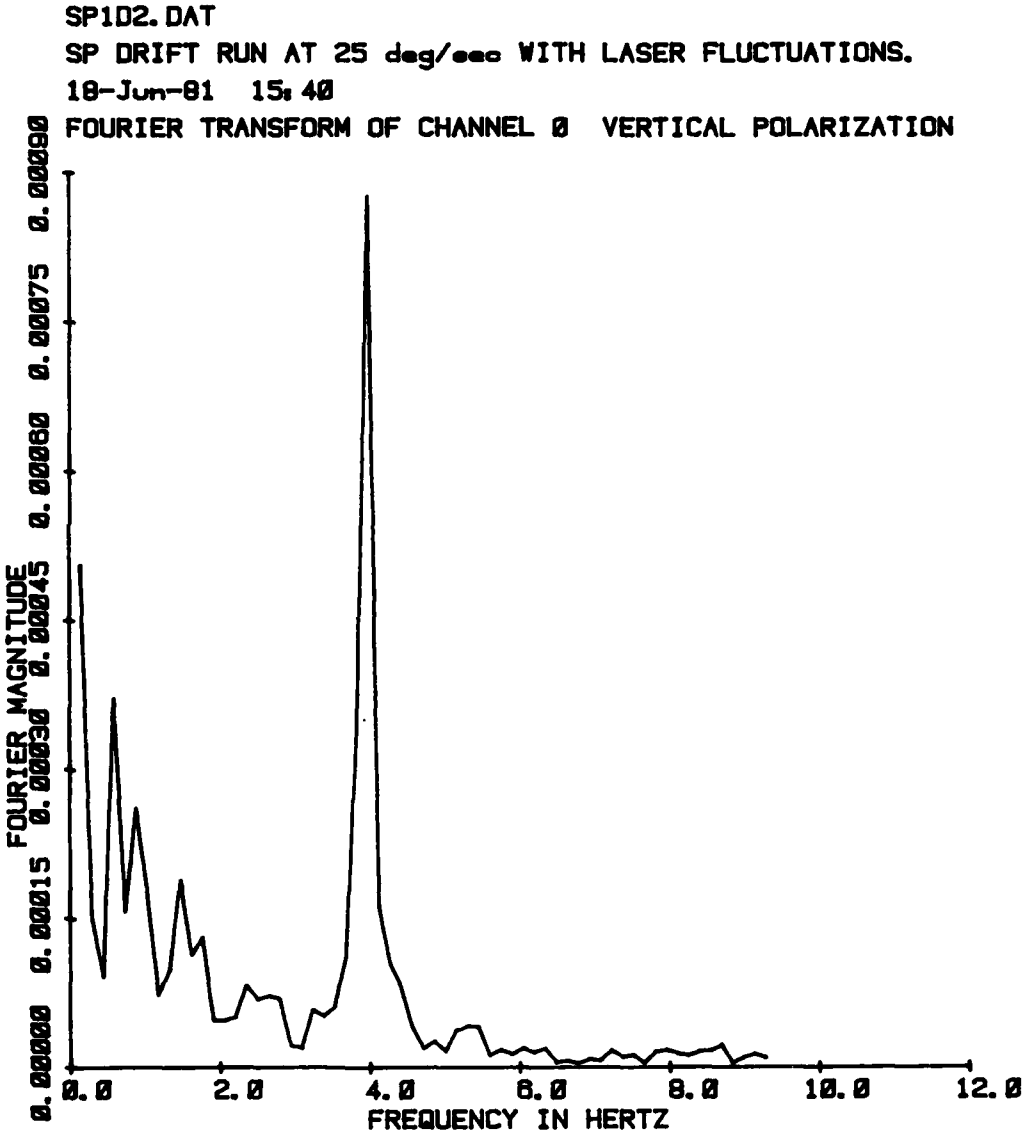

Figure 15. Power Spectral Density of Gyro Output

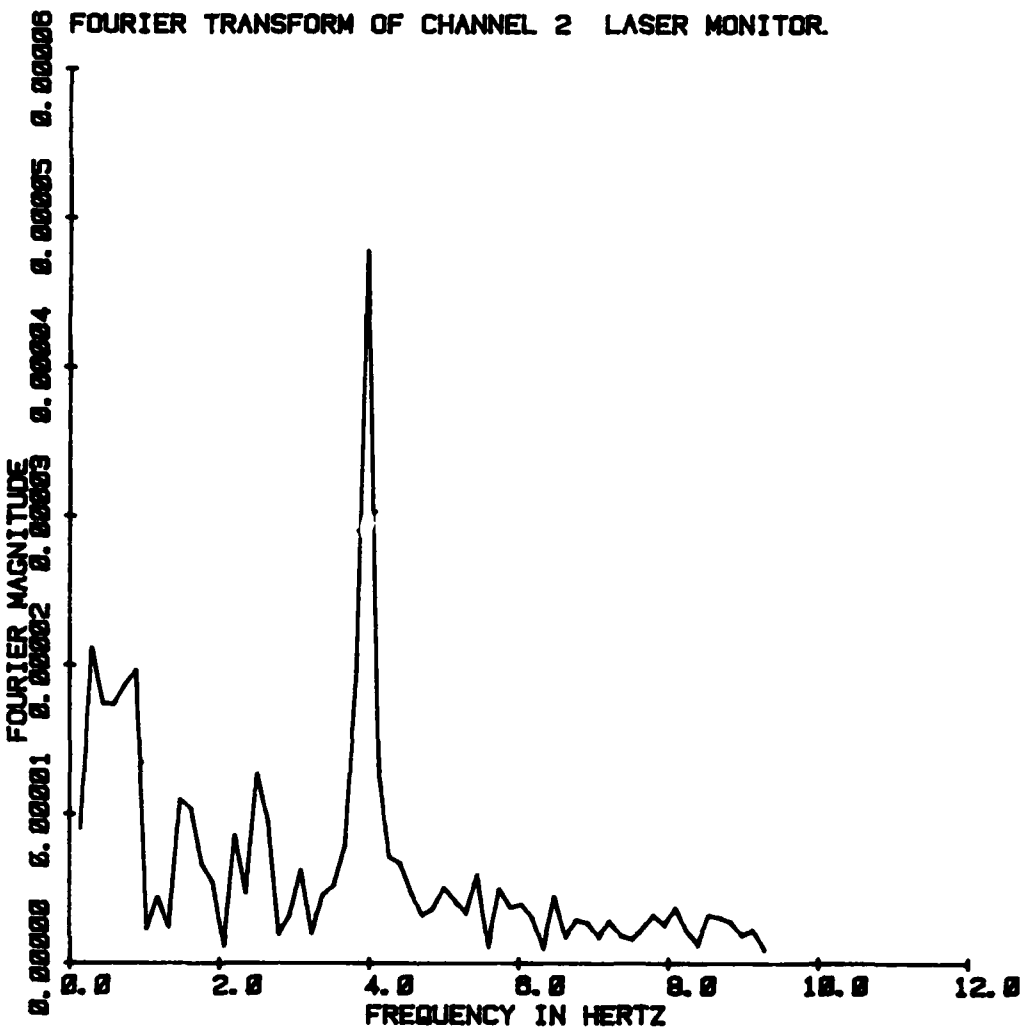

Figure 16. Power Spectral Density of Laser Output

We constructed a Faraday rotator/polarizer using materials suggested by the Naval Research Laboratory.[5] This isolator, shown in Figure 17, was instrumental in reducing overall gyro noise levels. Other techniques, such as improved optical component quality and spatial filtering of the gyro input, were also examined.

These improvements resulted in a significant decrease in system noise, which allowed backscattering from the fiber to become the most significant noise source. The fiber stretcher was implemented to decorrelate backscattering, allowing further improvement in the gyro performance. Both frequency swept (chirped) and continuous sine wave exertation for the PZT stretcher were evaluated. The most effective decorrelation was found to be in the 4.0 - 4.5 KHz region. A 1-centimeter diameter PZT cylinder with about 15V was used with 10 fiber turns. Figure 18 illustrates the before/after results in a drift run using the dual polarization gyro output. The RMS noise in the runs in Figure 18 show a factor of 31 improvement with the decorrelator on.

The gyro output characteristics using the noise reduction techniques described above are shown in Figure 19. This output compares favorably with the previous output, Figure 14. The scale factor change in the two figures is a result of neutral density filters in the gyro input portion of the experiment. At the time these data were taken, the input power was approximately 100 microwatts.

A long-term drift run is shown in Figure 20. Here the data are plotted with an expanded vertical scale, allowing more detailed examination of the noise. Aside from a turn-on transient, the data are relatively stable. The drift indicated by the portion of the plot after the stabilization is approximately 50 deg/hr/hr. This is a surprisingly good bias stability value for such a flexible experimental set-up.

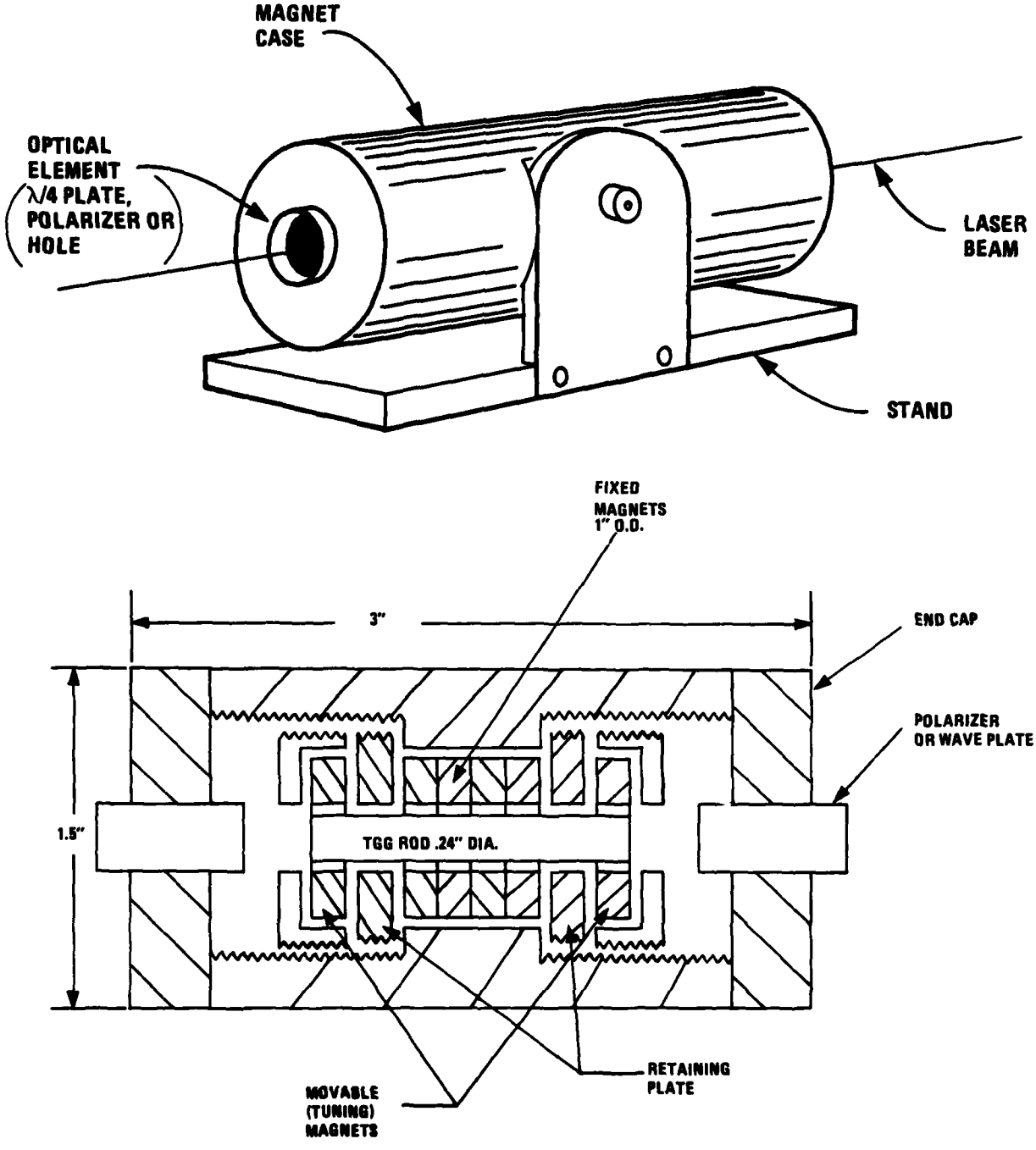

Figure 17. Faraday Rotator

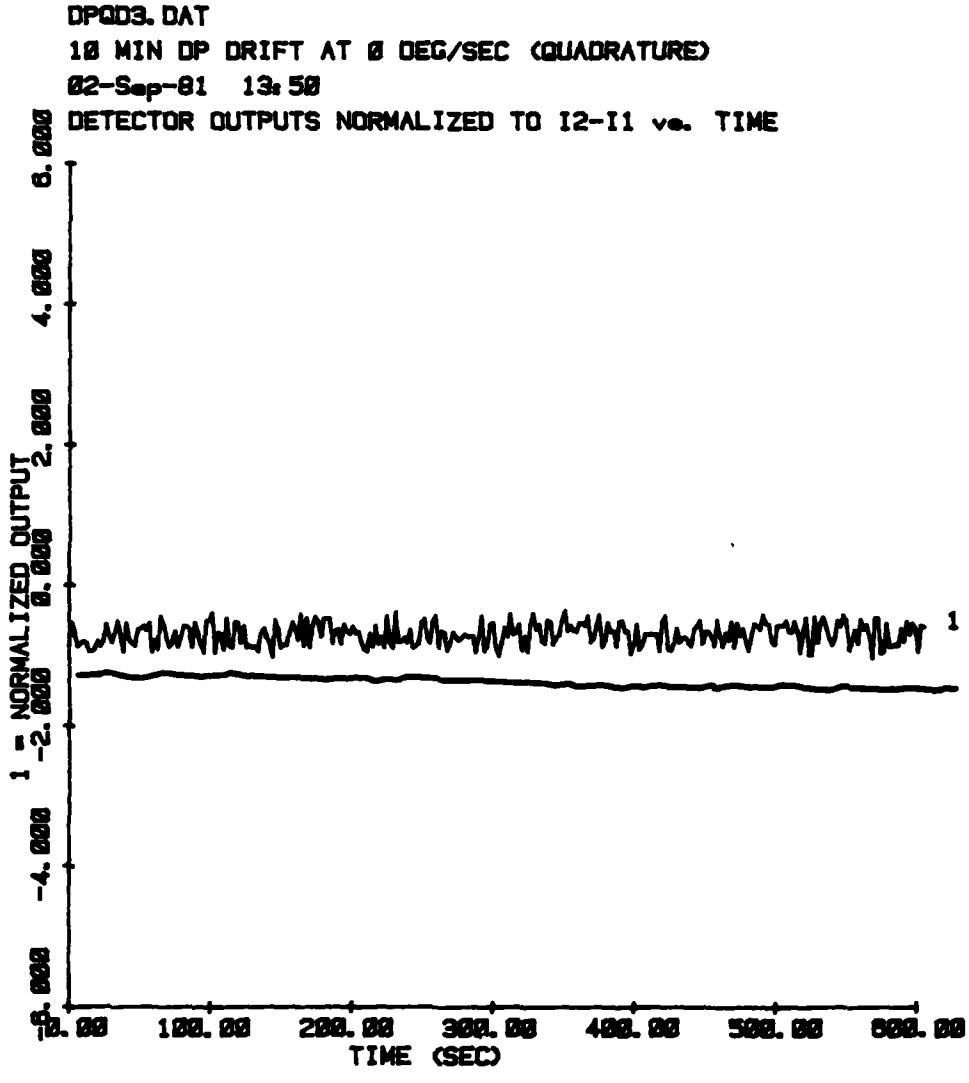

Figure 18. Comparison of Drift Run With (1) and Without (2) Chirped Decorrelator

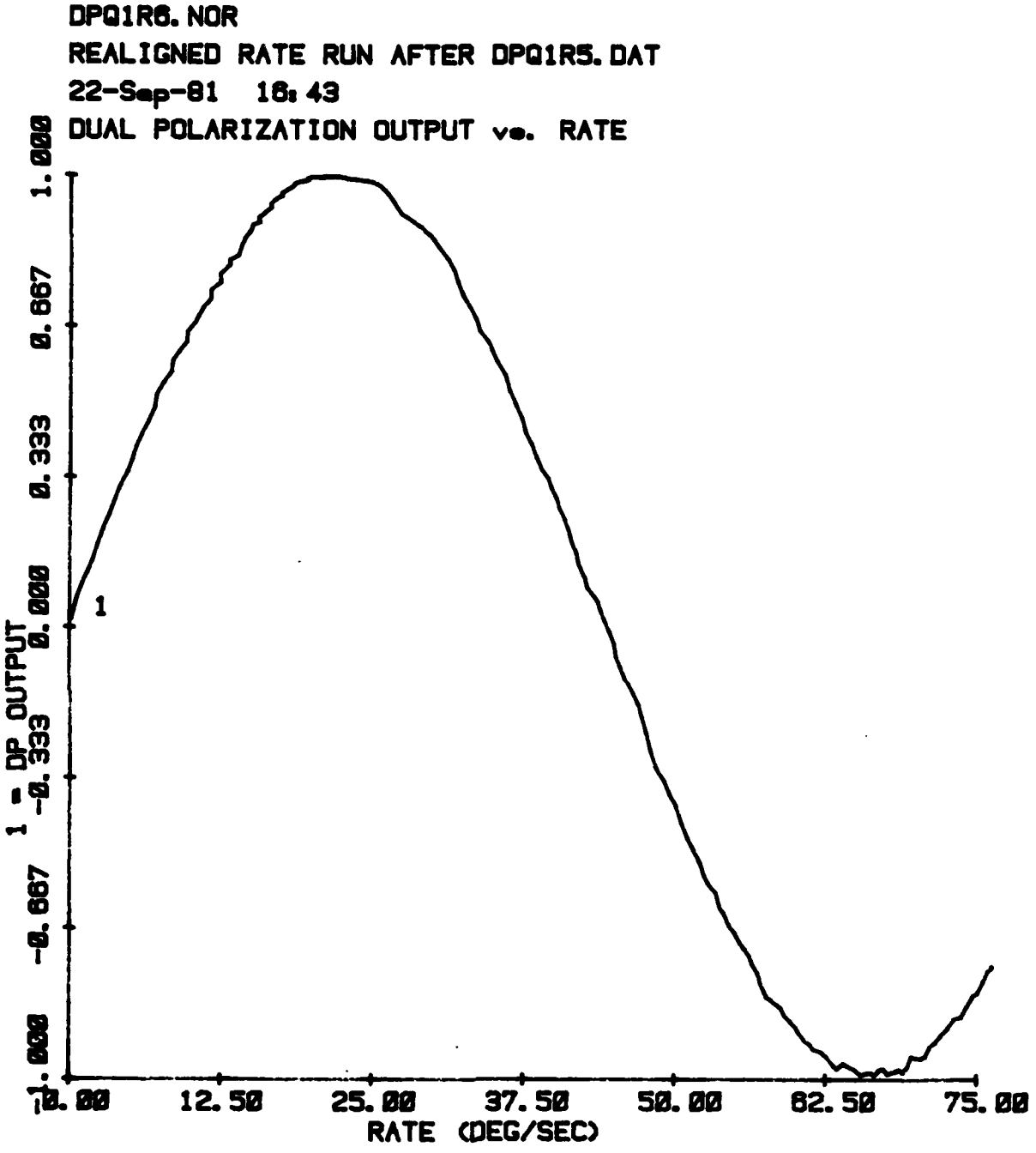

Figure 19. Dual Polarization Gyro Output After Noise Reduction

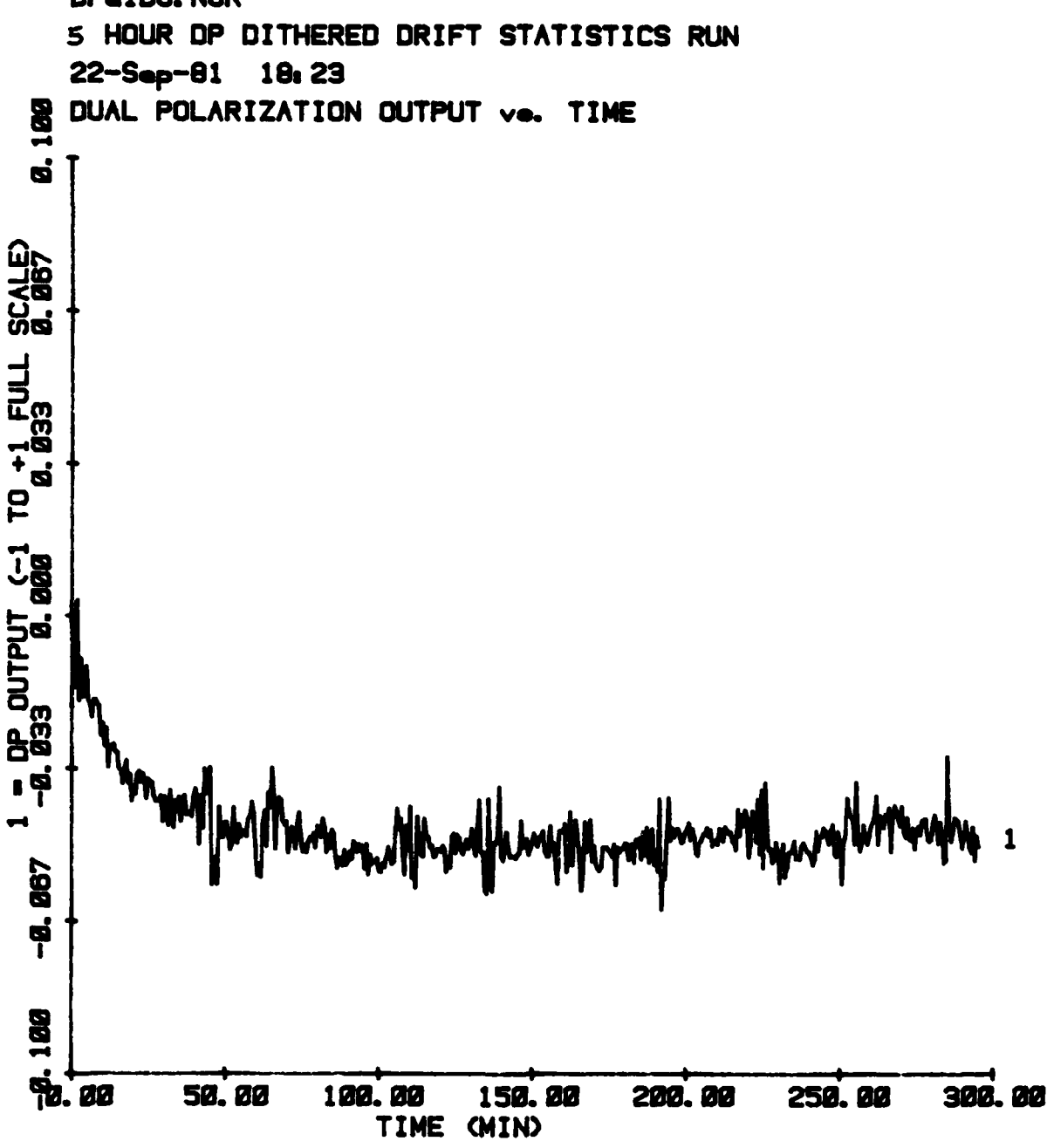

Figure 20. Long-Term Drift Run with Expanded Vertical Scale

The most important objective of this experimental effort was to demonstrate dual polarization gyro independence from phase modulator errors. It was hoped that the analytical predictions of Section 2 and the numerical modeling of Section 3 could be verified experimentally. To accomplish this it would be necessary to measure gyro bias while changing phase modulator settings. The principal factor in phase modulator stability is environmental temperature; this parameter was varied over a time period of about one hour, and the gyro drift recorded.

Figure 21 shows the temperature change of the Faraday cell housing as a function of time. In this example it was heated to about 33°C and allowed to cool. During the experiment, laser output power was also observed to fluctuate. This is plotted in the lower curve of Figure 21. A conventional gyro would be expected to respond (drift) in response to these perturbations. This is, in fact, what is observed in Figure 22. The curves labeled 0 and 2 are the two single polarization outputs of a gyro plotted on the same time scale shown in the previous figure.

Curve 1 in Figure 22 shows the dual polarization performance of this gyro. It is an order of magnitude more stable than the conventional (single) polarization gyro. This confirms the expectation of better drift performance for the dual polarization gyro.

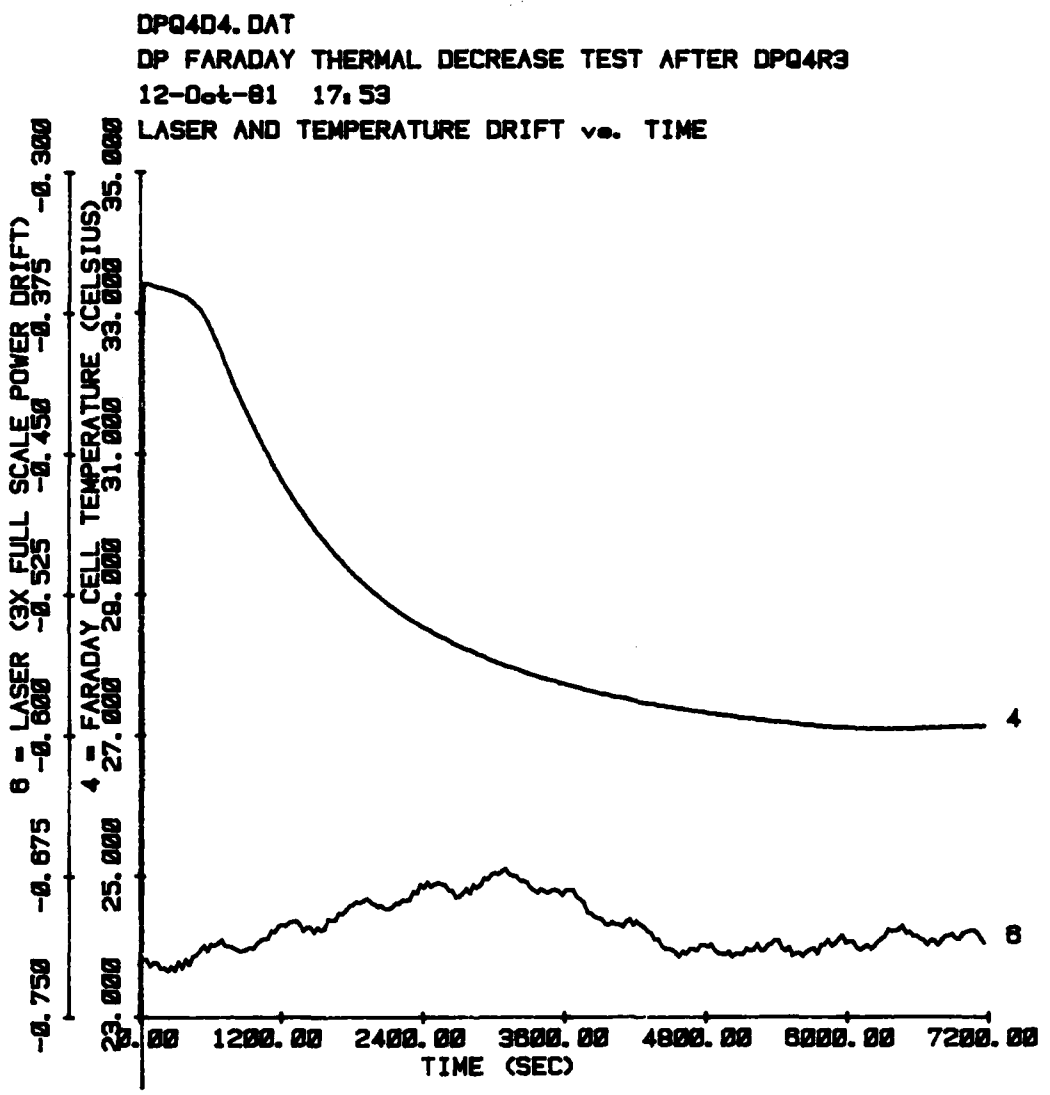

Figure 21. Faraday Cell Temperature and Laser Output Power Fluctuations vs Time During Drift Measurements

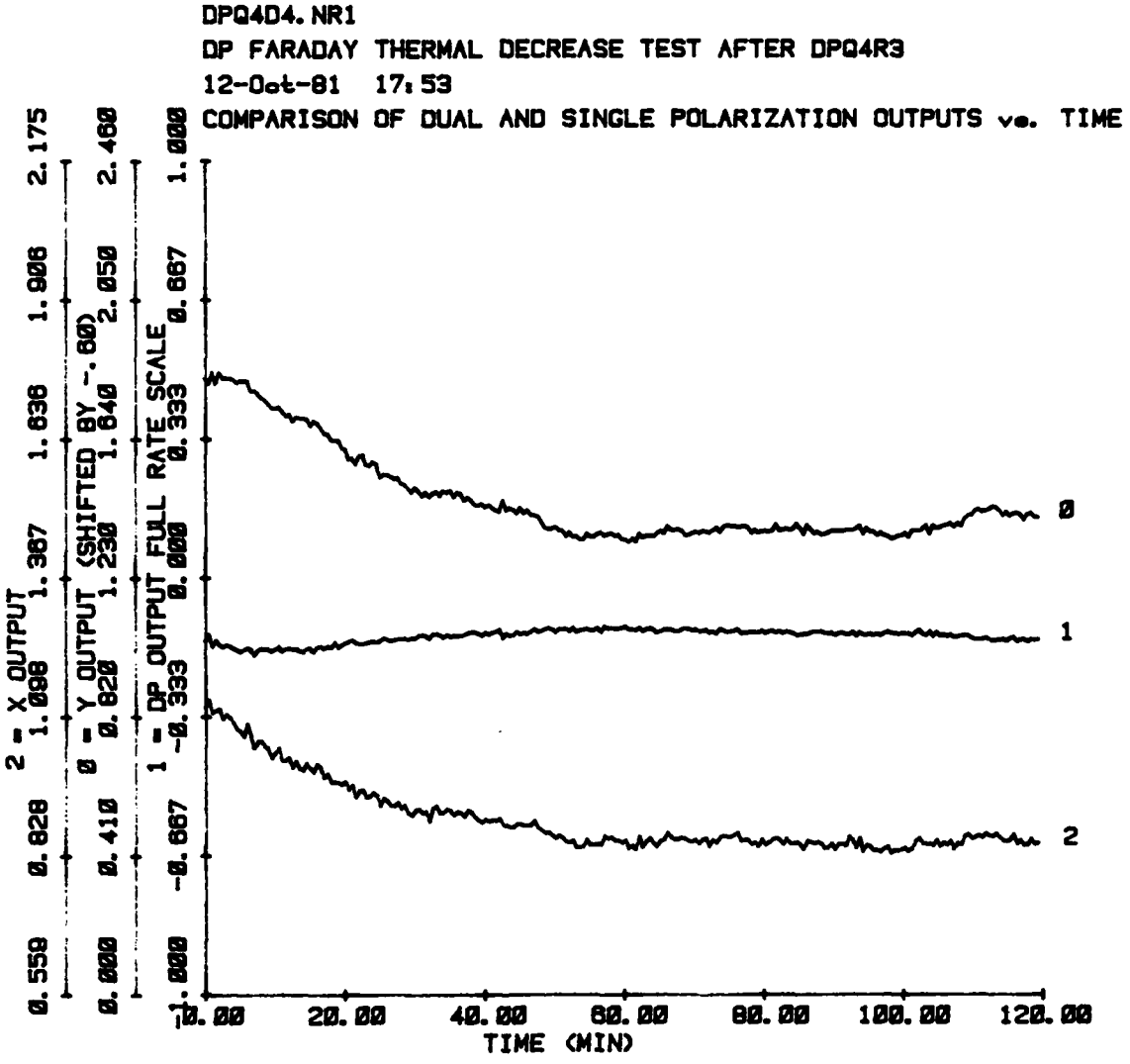

Figure 22. Single Polarization (curves 0, 2) and Dual Polarization (curve 1) Output Showing an Order of Magnitude Stability Improvement for Dual Polarization.

SECTION 5

REFERENCES

1. E.J. Post, "Sagnac Effect," Review of Modern Physics, vol. 19, no. 475, 1967.

2. B.H. Billings, "A Monochromatic Depolarizer," Optical Society of America, vol. 41, no. 12, December 1951. pp. 966-975.

3. M. Johnson, "Poincare Sphere Representation of Birefringent Networks," Applied Optics, vol. 20, no. 12, 15 June 1981. pp. 2075-2080.

4. H.C. Lefevre, "Single-Mode Fiber Fractional Wave Devices and Polarization Controller," Electronics Letters, vol. 16, no. 20, 25 September 1980. pp. 778-780.

5. Private Communication, Joseph Weller, Naval Research Laboratory.

APPENDIX A

SOFTWARE DETAILS

APPENDIX A

SOFTWARE DETAILS

Programs used for Fluke 1720A programming are included in this report to allow their use by other researchers, and to quantify the statistical measures of performance used in the experimental portions of this report.

DATRUN

This routine is a general-purpose, fast data acquisition routine that reads and stores up to 10 channels of 6-1/2 digit analog data at a rate up to 200 channels per second. The routine sets up the 7600-scanner/DVM-subsystem in its fastest acquisition mode. The number of channels read and the speed at which they will be read are under user control at run time. On command the program acquires data and stores them in temporary storage until the operator terminates the test or the storage space is exhausted. This read and store operation allows for the high-speed operation. At completion of the test, stored data are converted to real numbers and stored on the diskette in a permanent file. The data can then be viewed and analyzed using other routines. The listing of DATRUN follows below.

```
10!   DATRUN.BAS .... FAST DATA STORAGE ROUTINE
20!                PAUL BJORK, PROGRAMMER  3-30-81.
30!                VARIABLE CHANNEL INPUT NUMBER.
40!                VARIABLE SAMPLE AND BURST INTERVAL SET.
50!                CLOSES UPON DISPLAY TOUCH OR ARRAY OVERFLOW.
60!                USES RBYTE WBYTE STATEMENT
70!                IN 3 BYTE BINARY INPUT FORMAT.
80!                MAXIMUM SPEED—200 CHANNELS PER SECOND.
90!
100!         **      USES VIRTUAL ARRAY FILE  **
110!                     B$(0) CONTAINS FILE FORMAT INFO. NO. OF CHANNELS.
120!                     B$(1) CONTAINS TOTAL NUMBER OF BURSTS.
130!                     A(BURST,CHANNEL) CONTAINS VOLTAGE DATA.
140!                     TB(BURST) IS THE ELAPSED RUNNING TIME.
150!         **      DVM HIGH SPEED READING MODE      **
160!
170!        REVISION 2... DVM IS SET TO THE 2.5 VOLT RANGE.
180!             ALTER LINES 250 AND 870.  P. BJORK, 8/4/81.
190!             MULTIPLE BURST SEQUENCES POSSIBLE ON SAME FILE 8-14-81
200 COM Y
210 ES$=CHR$(27)+"["
220 IF Y=1 GOTO 1740          !GO DIRECTLY TO OUTPUT THE FILE!
230 DIM AD%(9%), A1(10)
240 K%=KEY \ ON KEY GOTO 1090
250 RF=1.!/8.      ! RF FOR 20 V SCALE IS 1. RF FOR 2.5 VOLT SCALE IS 1/8
260 K%=KEY
270 ES$=CHR$(27%)+"["
280!
290! SET UP WBYTE COMMAND STRING ARRAY.
300!
310 AD%(0%)=607%              ! ATN, UNT
320 AD%(1%)=544%+1%           ! ATN, MTA DVM
330 AD%(2%)=63%               ! ASCII "?" TRIGGERS DVM
340 AD%(3%)=575%              ! ATN, UNL DVM
350 AD%(4%)=544%+3%           ! MLA SCANNER
360 AD%(5%)=43%               ! ASCII "+" INCREMENTS SCANNER
370 AD%(6%)=40%               ! ARBITRARY TIME DELAYER
380 AD%(7%)=575%              ! ATN, UNL SCANNER
390 AD%(8%)=576%+1%           ! ATN, MTA DVM
400!
410 PRINT ES$+"2J";CPOS(3,1)
420 PRINT "DATRUN.BAS ....3 BYTE 2.5 V. RANGE HIGH SPEED DATA STORAGE ROUTINE."
430 PRINT
440 PRINT "PLEASE ENTER THE FOLLOWING:"
450 PRINT "      DATA FILE NAME. (<CR> to view a file) ";  \  INPUT FI$
460 IF FI$<>"" GOTO 480 ELSE Y=1              ! TO VIEW FILE
470 RUN
480 PRINT "      FILE HEADER. ";   \  INPUT FH$
490 PRINT "      STARTING CHANNEL, NUMBER OF CHANNELS. ";\ INPUT SC%,NC%
500 PRINT "      BURST INTERVAL(ms).   ";  \  INPUT TS
510 PRINT "      TOTAL BURST NUMBER.   ";  \  INPUT SZ$
520    IF SZ$="" THEN SZ%=300% ELSE SZ%=VAL(SZ$)    ! MAXIMUM ARRAY SIZE
530!
540! INITIALIZE THE VIRTUAL DATA FILE
550!
```

```
560 OPEN FI$ AS NEW DIM FILE 1 SIZE ((NC%+1%)*SZ%)/64%+2%
570 DIM #1, B$(0%) = 64%, A(SZ%,NC%)
580 DIM RA(NC%),IA%(SZ%*3%*NC%),TB(SZ%)
590 NC=NC%
600 B$(0%)=NUM$(NC)                    ! NUMBER OF CHANNELS.
610 B$(2%)=FI$                         ! FILE NAME
620 B$(3%)=FH$                         ! FILE HEADER.
630 B$(4%)=DATE$+'  '+TIME$
640!
650 PRINT ES$+'2J';ES$+'1p';CPOS(2,1)
660 PRINT "PRESS SCREEN TO INITIATE READINGS"
670 ON KEY GOTO 680  \ WAIT
680 K%=KEY \ RESUME 690
690 PRINT ES$+"2J";CPOS(2,1);"SCANNING CHANNELS ";SC%;" TO ";SC%+NC%-1;"."
700 PRINT CPOS(5,1);"DATA FILE NAME IS ";FI$;"."
710 PRINT CPOS(7,1); "PRESS SCREEN TO HALT."
720!
730! INITIALIZE METER AND SCANNER
740!            METER--FILTER BYPASS, REMOTE TRIGGER, VARIABLE SAMPLE
750!            SCANNER--SET LOWER AND UPPER INCREMENTAL BOUNDARIES
760!
770 INIT PORT 0
780 CLEAR @1
790 REMOTE @1@3
800!
810 IM%=NC%*3%-1% \ UP%=SC%+NC%-1
820 INIT PORT 0
830 PRINT @3%,"*,($,,)";               ! RESET AND CLEAR SCANNER
840 PRINT @3%,SC%;",,0"                ! SET CHANNEL BOUNDARIES
850 PRINT @3%,UP%;",,1";
860 PRINT @3%,SC%;","                  ! SET TO STARTING CHANNEL
870 PRINT @1,"VR2S2F1TOBQO!"           ! R1 IS 2.5 V RANGE. R2 IS 20 V RANGE.
880 WAIT 3000
890 PRINT ES$+'5m'; 'ACQUISITION IN PROGRESS.';
900 INPUT LINE @1,D1$
910!
920! PRINT "ELAPSED TIME:     0  MINUTES";
930! PRINT ES$+"16D";
940! T=TIME
950 FOR J%=0 TO SZ%-2%                 ! DO LOOP SET TO MAX SIZE
960   K3%=3%*NC%*J%
970   RBYTE (WBYTE AD%(0%..8%)) IA%(K3%..K3%+3%*NC%-1%);3%
980!
990   TB(J%)=TIME
1000!  PRINT USING "####.##",(TB(J%))/60;ES$+'7D';
1010   ON KEY GOTO 1090
1020   WAIT  TS-5
1030   OFF KEY
1040 NEXT J%
1050   J%=J%-1%                        ! REDUCE J% FOR NORMAL DO LOOP EXIT
1060!
1070! CONVERT DATA TO REAL, CLOSE FILE, AND INFORM ON FILE STATUS.
1080!
1090 K%=KEY
1100 IF K%=0% GOTO 1200
```

```
1110    PRINT ES$+'m';ES$+'2J'
1120    PRINT CPOS(3,3);'RESUME DATA ACQUISITION ON THIS FILE'
1130    PRINT CPOS(5,1);'TOUCH SCREEN FOR CHOICE'
1140    PRINT CPOS(7,7);'CONVERT EXISTING DATA'
1150    ON KEY GOTO 1160 \ WAIT FOR KEY
1160 K%=KEY
1170 OFF KEY
1180 IF K%>30 GOTO 1190
1182    PRINT ES$+'2J';CPOS(5,1);'RESUMING DATA ACQUISITION (5 SEC)'
1183    WAIT 5000
1184    PRINT ES$+'5m';CPOS(8,5);'ACQUISITION IN PROGRESS'
1185    RESUME 1040
1190 RESUME 1200
1200 JT=J%                                  ! JT IS TOTAL NO. OF BURSTS MINUS 1.
1205 ON CTRL/C GOTO 1340
1210 TO=TB(0%)
1220 PRINT ES$+'2J';ES$+'m';CPOS(3,1);"CONVERTING DATA."
1225 CLEAR @1@3
1230 FOR K%=0% TO JT
1240   K3%=3%*NC%*K%
1250   A(K%,NC%)=(TB(K%)-TO)/1000           ! BURST TIME IS ON THE NC% COLUMN.
1260   GOSUB 2060                           ! CONVERSION SUBROUTINE
1270   FOR J%=0 TO NC%-1%
1280     A(K%,J%)=RA(J%)
1290   NEXT J%
1300   PRINT CHR$(7);
1310 NEXT K%
1320 B$(1%)=NUM$(JT+1)                      ! NUMBER OF BURSTS.
1330 B$(5%)=NUM$(A(JT,NC%),"******.##")+" SECONDS TOTAL TIME"
1340 CLEAR @1@3
1350 CLOSE 1
1360 GOTO 1380
1370!
1380!  SUBROUTINE ASK FOR INSTRUCTIONS
1390!
1400 PRINT ES$+'2J';ES$+'m';CPOS(2,1);
1410 PRINT "KEY CLOSURE: DATA ACQUISITION STOPPED."
1420 PRINT  FI$ ;" IS FILLED AFTER ";
1430 PRINT JT+1;" BURSTS."
1440!
1450! CHOICE ENTRY POINT
1460!
1470 PRINT CPOS(5,1); "CHOOSE A FUNCTION."
1480! PRINT ES$+'1m';
1490 PRINT ES$+'5m';CPOS(6,6);'EXIT';CPOS(6,18);'VIEW';CPOS(6,30);'AGAIN'
1500 K%=KEY \ ON KEY GOTO 1510 \ ON CTRL/C GOTO 1620 \ WAIT FOR KEY
1510 K%=KEY \ RESUME 1520
1520 PRINT ES$+'m';
1530 IF K%=41 GOTO 1620                     ! THEN EXIT.
1540 IF K%<>49 GOTO 1570
1550 PRINT ES$+'p';                         ! RECYCLE TO A NEW DATA FILE.
1560 RUN
1570 IF K%=45 THEN PRINT ES$+'p' ELSE GOTO 1470
1580 Y=1                                    ! VIEW A FILE
1590 RUN
```

```
1600 PRINT ES$+'1p'
1610 GOTO 1470
1620!
1630 PRINT ES$+"p"
1640!
1650 END
1660!
1670! VIRTUAL FILE PRINTOUT SUBROUTINE
1680!          A(I,J) IS THE NUMERIC ARRAY
1690!          B$(K) IS THE FILE HEADER ARRAY
1700!                - B$(0) CNTAINS THE NUMBER OF COLUMNS IN STRING FORMAT
1710!                - B$(1) CONTAINS THE NUMBER OF ROWS
1720!          TB(J) IS THE RUNNING BURST TIME.
1730!
1740 Y=0 \ PRINT ES$+'p';ES$+'2J';CPOS(3,1)
1750 PRINT "ENTER VIRTUAL FILE NAME FOR LISTING.... "; \ INPUT FJ$ \ GOTO 1760
1760 ON CTRL/C GOTO  2030 \ ON KEY GOTO 2020
1770 OPEN FJ$ AS OLD DIM FILE 1
1780 DIM #1, B2$(6%) = 64%, A5(VAL(B2$(1)),VAL(B2$(0)))
1790 NC%=VAL(B2$(0)) \ NB%=VAL(B2$(1))
1800 PRINT
1810 PRINT 'FILENAME ';B2$(2)
1820 PRINT B2$(3)
1830 PRINT B2$(1);' BURSTS.'
1840 FOR I%=4% TO 5%
1850 PRINT B2$(I%)
1860 NEXT I%
1870 PRINT
1880 FOR I%=0 TO VAL(B2$(0))-1
1890    PRINT ' CHAN.';I%;
1900 NEXT I%
1910 PRINT "  TIME (sec.)" \ PRINT
1920 FOR I%=0% TO NB%-1%
1930 FOR J%=0% TO NC%-1%
1940     PRINT NUM$(A5(I%,J%),"S###.####");
1950 NEXT J%
1960 PRINT NUM$(A5(I%,NC%),"####.#")
1970 NEXT I%
1980 PRINT
1990 PRINT 'PRESS SCREEN TO CONTINUE.'
2000 ON KEY GOTO 2020 \ WAIT
2010 GOTO 2030
2020 K%=KEY \ RESUME 2030
2030 CLOSE 1
2040 PRINT ES$+'1p';CPOS(2,1);"DATRUN"; \ GOTO 1470
2050 !
2060 !         SUBROUTINE  3BYTE.BAS
2070 !
2080 !   VERSION 1.1       12/12/79        J.CHURCHILL
2090 !
2100 !          BASIC V1.0, FDOS V1.0
2110 !
2120 !   3BYTE WILL CONVERT AN INTEGER ARRAY < IA% > READ IN FROM
2130 ! THE 8502A IN HIGH SPEED READING MODE ( 3-BYTE BINARY TRANSFER ).
2140 !
```

```
2150 C1%=255%                                          ! CONSTANT FOR 1'S COMPLEMENT
2160 C2%=256%                                          ! CONSTANT FOR 2'S COMPLEMENT
2170 C1=16%/(10%*RF)                                   ! CONSTANT FOR BYTE 1
2180 C2=4096%/(10%*RF)                                 ! CONSTANT FOR BYTE 2 (2^12)
2190 C3=1048576/(10%*RF)                               ! CONSTANT FOR BYTE 3 (2^20)
2200 !
2210 FOR I%=K3% TO K3%+IM% STEP 3%
2220 !
2230 IA%(I%+2%)=IA%(I%+2%) AND C1%                     ! REMOVE EOI BIT
2240 IF IA%(I%) < 128% THEN IS%=1% \ GOTO 2290         ! CHECK FOR NEGATIVE READING
2250 IS%=-1%                                           ! SET SIGN TO NEGATIVE
2260 IA%(I%)=C1%-IA%(I%)                               ! COMPLEMENT BYTE 1
2270 IA%(I%+1%)=C1%-IA%(I%+1%)                         ! COMPLEMENT BYTE 2
2280 IA%(I%+2%)=C2%-IA%(I%+2%)                         ! COMPLEMENT BYTE 3
2290 IF IA%(I%) AND 32% THEN RA((I%-K3%)/3%)=0%\GOTO 2320 ! ERROR HAS OCCURED
2300 RA((I%-K3%)/3%)=(IA%(I%)/C1+IA%(I%+1%)/C2+IA%(I%+2%)/C3)*IS%
2310 !
2320 NEXT I%                                           ! LOOP
2330 RETURN
2340 END
```

DPDEV

In order to examine the gyro performance over long-term drift runs, a special acquisition program was developed. The routine acquires a burst of multiple channel data similarly to DATRUN. This burst is done at high data rate for a short time period, usually less than 10 seconds. These data are converted and statistically analyzed for the mean and sigma of each channel. These values are stored on file, and the program returns to acquire another burst of data. The collection of means will show the low-frequency drift character of the gyro, and the sigmas will show the high-frequency character of the gyro noise. Therefore, this acquisition and real time analysis yields a full bandwidth examination of the gyro output without prohibitively large data storage. The listing of DPDEV follows.

```
10!   DPDEV .... FAST DATA STORAGE ROUTINE
20!                PAUL BJORK, PROGRAMMER  3-30-81.
30!        VERSION 3 REVISION 1... DVM IS SET TO THE 2.5 VOLT RANGE.
40!        STREAMLINED FOR 'REAL TIME' STATISTICAL ANALYSIS.
45!        DUAL POLARIZATION VERSION 9/2/81
47!        DUAL POLARIZATION REVISION 1 9/10/81 J HANSE
50!        P. BJORK, 8/4/81.
60!
70 ES$=CHR$(27)+"["
80 J%=4%
90 DIM AD%(9%), A1(10),MN(J%),TN(1%),SF(J%),NS(J%),S(1%),SS(1%),S1(1%),S2(1%)
100 ON CTRL/C GOTO 1240
110 ON ERROR GOTO 1240
120 RF=1.      ! RF FOR 20 V SCALE IS 1.
130 GOSUB 1320   ! 3BYTE INITIALIZATION
140 ST$='S##.#####'
150 L1=1E-5
160 KE%=KEY
170!
180! SET UP WBYTE COMMAND STRING ARRAY.
190!
200 AD%(0%)=607%              ! ATN, UNT
210 AD%(1%)=544%+1%           ! ATN, MTA DVM
220 AD%(2%)=63%               ! ASCII "?" TRIGGERS DVM
230 AD%(3%)=575%              ! ATN, UNL DVM
240 AD%(4%)=544%+3%           ! MLA SCANNER
250 AD%(5%)=43%               ! ASCII "+" INCREMENTS SCANNER
260 AD%(6%)=40%               ! ARBITRARY TIME DELAYER
270 AD%(7%)=575%              ! ATN, UNL SCANNER
280 AD%(8%)=576%+1%           ! ATN, MTA DVM
290!
300 PRINT ES$+"2J";CPOS(3,1);
310 PRINT "DPDEV .... DATA ACQUISITION AND REAL TIME STATISTICAL ANALYSIS"
315 PRINT '          FOR DUAL POLARIZATION GYRO DRIFT TESTING'
320 PRINT CPOS(5,6);'ENTER FILE NAME                ';\ INPUT FI$
340 PRINT CPOS(7,12);'FILE HEADER            ';\ INPUT FH$
350 PRINT CPOS(8,12);'STARTING CHANNEL       ';\ INPUT SC%
360 PRINT CPOS(9,12);'The input channels are assumed to be ';SC%;' and ';SC%+1%
370 PRINT CPOS(10,12);'BURSTS PER CYCLE       ';\ INPUT NB%
380 PRINT CPOS(11,12);'NUMBER OF CYCLES       ';\ INPUT CY%
390!
500! INITIALIZE THE VIRTUAL DATA FILE
510!
515    NC%=2%
520 OPEN FI$ AS NEW DIM FILE 1 SIZE (5%*CY%)/64%+2%
530    DIM #1, B$(6%) = 64%, A(CY%,4%)
540    DIM RA(NC%),IA%(NB%*3%*NC%)
550    B$(0%)=NUM$(4%)                    ! NUMBER OF CHANNELS STORED ON FILE.
560    B$(2%)=FI$
570    B$(3%)=FH$
580    B$(4%)=DATE$+"  "+TIME$
590!
600! INITIALIZE METER AND SCANNER
610!           METER--FILTER BYPASS, REMOTE TRIGGER, VARIABLE SAMPLE
620!           SCANNER--SET LOWER AND UPPER INCREMENTAL BOUNDARIES
```

```
630!
640 INIT PORT 0
650 CLEAR @1
660 REMOTE @1@3
670 IM%=NC%*3%-1%
680 UP%=SC%+NC%-1              ! UPPER BOUND
690 INIT PORT 0
700 PRINT @3%,"*,($,,)";                ! RESET AND CLEAR SCANNER
710 PRINT @3%,SC%;",,0"                 ! SET CHANNEL BOUNDARIES
720 PRINT @3%,UP%;",,1";
730 PRINT @3%,SC%;","                   ! SET TO STARTING CHANNEL
740 PRINT @1,"VR2SOF1TOB00!"            ! R1 IS 2.5 V RANGE. R2 IS 20 V RANGE.
750 INPUT LINE @1,D1$
760 PRINT CPOS(13,1);' TIME (MIN)           DET. 1';TAB(65%);'DET. 2'
765 PRINT CPOS(14,19);'MEAN       SIGMA                  MEAN       SIGMA'
770 PRINT
780 TO=TIME
790!
800! CYCLE ACQUISITION AND ANALYSIS LOOP
810!
820 ON KEY GOTO 1170
830 FOR L%=0% TO CY%-1%
840   A(L%,0%)=(TIME-TO)/(1000*60)      ! TIME STORED IN MINUTES
845   FOR J%=0% TO 1%
850     S(J%)=0.
860     SS(J%)=0.
865   NEXT J%
870   OFF KEY
880   FOR K%=0% TO NB%-1%
890     K3%=3%*NC%*K%
900     RBYTE (WBYTE AD%(0%..6%)) IA%(K3%..K3%+3%*NC%-1%);3%
910   NEXT K%
920   ON KEY GOTO 1170
930   FOR K%=0% TO NB%-1%
940     K3%=3%*NC%*K%
950     GOSUB 1410                          ! CONVERSION SUBROUTINE
960!    FOR J%=1 TO NC%
970!      NS(J%)=(RA(J%-1%)-MN(J%))/SF(J%)              ! SINUSOIDS
980!    NEXT J%
1015    FOR J%=0% TO 1%
1020      S(J%)=S(J%)+RA(J%)
1040      SS(J%)=SS(J%)+RA(J%)*RA(J%)
1045    NEXT J%
1050  NEXT K%
1053  PRINT USING '###.##',A(L%,0%),
1055  FOR J%=0% TO 1%
1060    S1(J%)=S(J%)/NB%
1070    S2(J%)=SQR((SS(J%)/NB%)-S1(J%)^2)
1080    A(L%,1%+2*J%)=S1(J%)                ! 1,3 ARE MEAN OF DET 1 AND 2
1090    A(L%,2%+2*J%)=S2(J%)                ! 2,4 ARE SIGMA OF DET 1 AND 2
1100    PRINT USING ST$,S1(J%);' ';S2(J%),
1103  NEXT J%
1105  PRINT
1110  IF KE%<>0% GOTO 1220
1120 NEXT L%
```

```
1130!
1140 L%=L%-1%                              ! FOR NORMAL DO LOOP EXIT
1150 GOTO 1210
1160!
1170 PRINT 'KEY CLOSURE: ANALYSIS WILL CONTINUE TO FINISH CYCLE.'
1180 KE%=KEY
1190 RESUME
1200!
1210! CLOSE FILES AND END
1220 B$(1%)=NUM$(L%)                       ! NUMBER OF CYCLES
1230 B$(5%)=NUM$(A(L%,0%))+' MINUTES TOTAL TIME'
1240 CLEAR @1@3
1250 CLOSE 1
1260 IF ERR<> 0 THEN PRINT 'ERROR '+ERR$' OCCURED ON LINE '+ERL  \ GOTO 1270
1270 CLOSE 1
1280 END
1290 !
1300 !         SUBROUTINE  3BYTE INITIALIZATION.
1310 !
1320 C1%=255%                                          ! CONSTANT FOR 1'S COMPLEMENT
1330 C2%=256%                                          ! CONSTANT FOR 2'S COMPLEMENT
1340 C1=16%/(10%*RF)                                   ! CONSTANT FOR BYTE 1
1350 C2=4096%/(10%*RF)                                 ! CONSTANT FOR BYTE 2 (2^12)
1360 C3=1048576/(10%*RF)                               ! CONSTANT FOR BYTE 3 (2^20)
1370 RETURN
1380!
1390!           SUBROUTINE 3BYTE CONVERSION
1400!
1410 FOR I%=K3% TO K3%+IM% STEP 3%
1420!
1430    IA%(I%+2%)=IA%(I%+2%) AND C1%                  ! REMOVE EOI BIT
1440    IF IA%(I%) < 128% THEN IS%=1% \ GOTO 1490      ! CHECK FOR NEGATIVE READING
1450    IS%=-1%                                        ! SET SIGN TO NEGATIVE
1460    IA%(I%)=C1%-IA%(I%)                            ! COMPLEMENT BYTE 1
1470    IA%(I%+1%)=C1%-IA%(I%+1%)                      ! COMPLEMENT BYTE 2
1480    IA%(I%+2%)=C2%-IA%(I%+2%)                      ! COMPLEMENT BYTE 3
1490    IF IA%(I%) AND 32% THEN RA((I%-K3%)/3%)=0%\GOTO 1520 ! ERROR HAS OCCURED
1500    RA((I%-K3%)/3%)=(IA%(I%)/C1+IA%(I%+1%)/C2+IA%(I%+2%)/C3)*IS%
1510 !
1520 NEXT I%                                           ! LOOP
1530 RETURN
1540 END
```

DPSTAT

This is a simple statistical analysis package. The data is input from the diskette. The routine can accept data from either DATRUN or DPDEV. The routine spools through the data and calculates the mean, sigma, maximum value and minimum value of each channel selected by the operator. These results are output to the printer. The routine then goes back and calculates a best fit straight line for the data using time as the independent variable, removes the line from the data, and calculates the residue. The residue, slope, and intercept are output to the printer. The units of the channels are preserved, so if the data were stored as volts every 10 seconds, the slope would be in volts per second and all the other outputs would be in volts

```
10! DPSTAT....DUAL POLARIZATION STATISTICAL DATA ANALYSIS ROUTINE.
20!           PAUL BJORK, PROGRAMMER.
30!           VERSION 1, REVISION 3, 8/5/81.
40!           DUAL POLARIZATION VERSION 9/10/81 JOEL HANSE
50!      FUNCTIONS:
60!        1. CALCULATES MEAN AND SIGMA ON CHANNEL IN A DATRUN TYPE FILE
70!        2. REMOVES A LEAST SQUARES STRAIGHT LINE.
80!        3. CALCULATES MEAN AND SIGMA OF RESIDUAL.
90!
100 ES$=CHR$(27)+"["
105 CH$=ES$+"H"+ES$+"2J"     ! CLEAR SCREEN AND HOME
106 LF$=CHR$(10)             ! LINE FEED
107 FF$=CHR$(12)             ! FORM FEED
108 OPEN "KB0:" AS NEW FILE 4
109 OPEN "KB1:" AS NEW FILE 5
110 PRINT CH$;CPOS(3,1);
120 ON ERROR GOTO 1030
130 ON CTRL/C GOTO 1030
140 J%=5%
150 DIM S(J%),SS(J%),NC%(J%),YX(J%),YM(J%),SX(J%),XX(J%),XY(J%),M(J%),B(J%)
160 ST$="S##.#####"
170!
180 PRINT ES$+"2J";CPOS(3,1);
190 PRINT "DPSTAT....DUAL POLARIZATION STATISTICAL DATA ANALYSIS ROUTINE."
200 PRINT
210 PRINT "          This routine performs three functions"
220 PRINT "            1. Calculates mean and sigma of any channel of a"
230 PRINT "                  standard (DATRUN) type virtual data file"
240 PRINT "            2. Removes least squares straight line"
250 PRINT "            3. Calculates mean and sigma of residual"
260 PRINT "          Items 2 and 3 can be disabled on command"
270 PRINT CPOS(14,5);"ENTER DATA FILE NAME.   "; \ INPUT FI$
280   OPEN FI$ AS OLD DIM FILE 1
290     DIM #1,B$(6%)=64%,A(VAL(B$(1%)),VAL(B$(0%)))
300     NB%=VAL(B$(1%))
320 PRINT CH$;CPOS(5,1);"FILE  ";FI$;"  CONTAINS  ";NB%-1%;" DATA POINTS"
330 PRINT CPOS(7,1);"FOR PARTIAL FILE DATA ANALYSIS ENTER"
340 PRINTCPOS(8,5);"LINE NUMBER OF FIRST DATA POINT TO CONSIDER "
350 PRINTCPOS(9,5);"AND NUMBER OF POINTS TO ANALYZE              ";
360 INPUT FP%,N
365 IF FP%+N>NB% GOTO 330
367 LP%=FP%+N-1
370 PRINT CPOS(11,1);"ENTER X AXIS CHANNEL FOR LEAST SQUARES LINE REMOVAL ";
375 PRINT CPOS(12,5);"C/R IMPLIES NO LEAST SQUARES LINE REMOVAL      ";
380   INPUT XC$
385 PRINT CH$;
390   IF XC$<>"" THEN XC%=VAL(XC$) \ GOTO 420
400   XC%=-1%
410 PRINT CPOS(7,1);"CALCULATING ONLY RAW DATA STATISTICS."
420 PRINT CPOS(8,5);"   ENTER COLUMNS TO BE ANALYZED "; \ INPUT NC$
430   CT%=LEN(NC$)
440   FOR I%=1% TO CT%
450     NC%(I%)=VAL(MID(NC$,I%,1%))
460   NEXT I%
470 GOSUB 1400                          ! ZERO ARRAYS
```

```
490 PRINT
500 PRINT CPOS(11,5);'CALCULATING MEAN AND SIGMA ON FILE ';FI$
510 FOR I%=FP% TO LP%
520    FOR J%=1% TO CT%
530       CN%=NC%(J%)
540       Y=A(I%,CN%)
550       GOSUB 1250                    ! CALCULATE SUMS
560    NEXT J%
570 NEXT I%
580!
582 PRINT CH$;
584 FOR IO= 4 TO 5
586 PRINT#IO,LF$;LF$;LF$;LF$;LF$
590 PRINT#IO,'          STATISTICS ON DATA FILE ';FI$;'.';LF$;LF$;LF$
610 PRINT#IO,'COLUMN NO.     MEAN          SIGMA          MINIMUM        MAXIMUM'
620 PRINT#IO
630 FL%=1%                              ! FLAG: PRINT MAX AND MIN.
640 GOSUB 1100                          ! PRINT RESULTS.
642 NEXT IO
650 IF XC%=-1% GOTO 1010                ! STOP IF NO STRAIGHT LINE FIT DESIRED.
660!
670! CALCULATE STRAIGHT LINE LEAST SQUARES FIT.
680!
685 GOSUB 1400                          ! ZERO ARRAYS AGAIN FOR STRAIGHT LINE FIT
690 PRINT CH$;CPOS(11,5);'CALCULATING STRAIGHT LINE FIT.'
700 FOR I%=FP% TO LP%
710    FOR J%=1% TO CT%
720       CN%=NC%(J%)
730       X=A(I%,XC%)            ! X AXIS CHANNEL.
740       Y=A(I%,CN%)
750       GOSUB 1250                    ! CALCULATE SUMS.
760       GOSUB 1330                    ! CALCULATE LINE SUMS.
770    NEXT J%
780 NEXT I%
790 FOR J%=1% TO CT%
800    M(J%)=(XY(J%)-SX(J%)*S(J%)/N)/(XX(J%)-(SX(J%)^2)/N)   ! SLOPE.
810    B(J%)=(S(J%)-M(J%)*SX(J%))/N                          ! Y INTERCEPT.
820 NEXT J%
830 PRINT
840!
850! CALCULATE STATISTICS ON RESIDUE.
860!
870 GOSUB 1400                          ! ZERO ARRAYS
880 FOR I%=FP% TO LP%
890    FOR J%=1% TO CT%
900       CN%=NC%(J%)
910       Y=A(I%,CN%)-(M(J%)*A(I%,XC%)+B(J%))  ! REMOVE LINE FROM Y POINT
920       GOSUB 1250                    ! CALCULATE SUMS.
930    NEXT J%
940 NEXT I%
950 PRINT CH$;
952 FOR IO = 4 TO 5
954 PRINT #IO,LF$;LF$;LF$;LF$
960 PRINT#IO, '    RESIDUE AND EXTRACTED LEAST SQUARES LINE STATISTICS.'
970 H$='COLUMN NO.     MEAN          SIGMA          SLOPE          Y INTERCEPT'
```

```
972 PRINT #IO,H$
980 GOSUB 1100
990 PRINT#IO, 'CALCULATIONS COMPLETED ON FILE '$FI$'.'
992 NEXT IO
1000!
1010! CLOSE FILES AND END OF PROGRAM
1020!
1030 IF ERR<>0 THEN PRINT 'ERROR '$ERR$'OCCURED ON LINE '$ERL$'.'
1040 CLOSE 1,4,5
1050 END
1060!
1070!
1080! CALCULATE MEAN AND SIGMA, PRINTOUT ROUTINE.
1090!
1100 FOR J%=1% TO CI%
1110    CN%=NC%(J%)
1120    S1=S(J%)/N
1130    S2=SQR((SS(J%)/N)-S1^2)
1140    PRINT #IO
1150    PRINT #IO,CN%;"         ";
1160    PRINT #IO,USING ST$,S1;TAB(26);S2;TAB(40);
1170    IF FL%=1% THEN PRINT#IO,USING ST$,YM(CN%);TAB(54);YX(CN%)\GOTO 1190
1180    PRINT#IO, USING ST$, M(J%);TAB(54);B(J%)
1190 NEXT J%
1200 PRINT#IO
1210 RETURN
1220!
1230! SUBROUTINE CALCULATE SUMS.
1240!
1250    S(J%)=S(J%)+Y                    ! SUM.
1260    SS(J%)=SS(J%)+Y^2                ! SUM OF SQUARES.
1270    IF YX(CN%)<Y THEN YX(CN%)=Y      ! MAXIMUM VALUE.
1280    IF YM(CN%)>Y THEN YM(CN%)=Y      ! MINIMUM VALUE.
1290 RETURN
1300!
1310! SUBROUTINE CALCULATE LINE SUMS.
1320!
1330    SX(J%)=SX(J%)+X          ! X SUM
1340    XY(J%)=XY(J%)+X*Y        ! XY PRODUCT SUM
1350    XX(J%)=XX(J%)+X^2        ! X AXIS SUM OF SQUARES.
1360 RETURN
1370!
1380! SUBROUTINE ARRAY ZEROING AND INITIALIZATION
1390!
1400 FOR J%=1% TO CI%
1410    FL%=0%
1420    S(J%)=0.                 ! INITIALIZATION
1430    SS(J%)=0.
1440    SX(J%)=0.
1450    XX(J%)=0.
1460    XY(J%)=0.
1470    CN%=NC%(J%)
1480    YX(CN%)=A(0%,CN%)
1490    YM(CN%)=A(0%,CN%)
1500 NEXT J%
```



```
1510 RETURN
1520 END
```

RATMAX

This simple routine spools through a data file that has been generated by DATRUN and determines the maximum and minimum values for each channel. The results are printed out and also stored on diskette for later use. This routine is particularly useful in determining the intensity scale factor of the gyro.

Program RATMAX will normalize any dual polarization data file stored as two single polarization detector outputs to the dual polarization mode I2-I1, and store the normalized data with time on an output file with a .NOR extension. Full rate scale is normalized to the sinusoidal -1 to +1 for easy computational reference.

```
10! RATMAX...ROUTINE PACKAGE TO FIND MAX AND MIN OF FIBER GYRO RATE ANGLE FILES
20!     REVISION 1, PROGRAMMER PAUL BJORK, 10-2/81.
30!     SUBROUTINES:
40!         LIMITS....RATE RUN SCALING LIMIT CALCULATION.
70!     MULTIDETECTOR DATA INPUT FILE FORMAT--'DATRUN', EXTENSION '.DAT'.
90!
100!          INPUT.DAT      OUTPUT.ANG      CHANNEL DESCRIPTION
110!             0              0            Rate or other.
120!             2              1            Horizontal Polarization angle.
130!             1              2            Vertical Polarization angle.
140!          Last              3            Elapsed time
150!
160 ES$=CHR$(27)+"["
165 ON CTRL/C GOTO 510
170 DIM F(8%,1%),SF(4%),MN(4%),MX(4%)
175 PRINT ES$+"2J"
180 PRINT CPOS(3%,1%);"RATMAX....RATE ANGLE SCALING LIMITS ROUTINE."
190 PRINT CPOS(5,5);"ENTER DATRUN RATE DATA FILE NAME";
200   INPUT FI$
210   Y%=INSTR(1%,FI$,".")
220   FO$=LEFT(FI$,Y%-1%)+".NOR"
225 PRINT CPOS(6,8);"ENTER FIRST DETECTOR COLUMN NUMBER (RATE=1,DRIFT=0) ";
227   INPUT SC%
230 PRINT CPOS(7,5);"ENTER DATRUN LIMITS FILE NAME";
240   INPUT FR$
245   IF FR$="" THEN FR$=FI$
250   Y%=INSTR(1%,FR$,".")
260   IF Y%=0% THEN Y%=LEN(FR$)+1%
270   FR$=LEFT(FR$,Y%-1%)
280 ON ERROR GOTO 430
290   OPEN FR$+".MXM" AS OLD DIM FILE 6       ! TEST FOR LIMITS FILE.
300     DIM #6,FF$(6%)=64%,FD(10%,5%) ! JUMP TO 430 IF NO EXISTING LIMITS FILE.
310! ON ERROR GOTO 510
320 GOSUB 4000              ! NORMALIZATION
360!
370! PROGRAM COMPLETED: HOUSECLEAN.
380!
390 CLOSE 1,2,5,6
395 PRINT CPOS(12%,5%);
400 PRINT "RATE ANGLE FILE ";FO$;" HAS BEEN FILLED AND CLOSED."
410 END
420!
430! LIMITS FILE ERROR POINT
440!
450 IF ERR <> 305 GOTO 510            ! ERROR 305 IS NO EXISTING FILE ON DEVICE
460 RESUME 465
465 PRINT CPOS(7%,5%);
468 PRINT "NO AVAILABLE LIMITS FILE...CALCULATING NEW SCALING RATIOS."
470 GOSUB 2000                        ! CALCULATE NEW LIMITS FILE.
480 GOTO 540
500!
510! ERROR NOTIFICATION
520!
530 PRINT "ERROR NUMBER ";ERR;" HAS OCCURED ON LINE ";ERL;"."
540 CLOSE 1,2,5,6
```

```
550 END
5o0!
2000! SUBROUTINE LIMITS....DETERMINES SCALING LIMITS FROM A
2010!                      RATE RUN FOR USE BY THE 'ANGLE' SUBROUTINE.
2020!     INPUT FILENAME IS IN 'DATRUN' FORMAT WITH A '.DAT' EXTENSION.
2030!     OUTPUT FILE IS 'Raterun filename.MXM' ON THE SAME FLOPPY DISC.
2130!
2145 CN=0.    ! .2                  ! FILTER CONSTANT.
2150 OPEN FR$+'.DAT' AS OLD DIM FILE 5
2160    DIM #5,B5$(6%)=64%,A5(VAL(B5$(1%)),VAL(B5$(0%)))
2170 FR$=FR$+'.MXM'
2180 OPEN FR$ AS NEW DIM FILE 6
2190    DIM #6,FF$(6%)=64%,FD(9%,5%)        !9 OR 10?
2200 NB%=VAL(B5$(1))
2210 NC%=VAL(B5$(0))
2240 FOR J%=SC% TO 1%+SC%
2250    T1=A5(0%,J%)                  ! INITIALIZE MAX AND MIN.
2260    MX(J%)=T1
2270    MN(J%)=T1
2290 NEXT J%
2300! FILTER AND LIMITS CALCULATION LOOP.
2310!
2320 FOR I%=0% TO NB%-1%
2330    FOR J%=SC% TO 1%+SC%
2340       F(J%,1%)=A5(I%,J%)
2360       IF MX(J%)<F(J%,1%) THEN MX(J%)=F(J%,1%)    ! TEST FOR MAXIMUM.
2370       IF MN(J%)>F(J%,1%) THEN MN(J%)=F(J%,1%)    ! TEST FOR MINIMUM.
2380    NEXT J%
2390 NEXT I%
2400!
2410! WRITE DATA TO THE OUTPUT FILE.
2420!
2425 PRINT CPOS(11%,10%); '   CHANNEL                MIN                MAX'
2430 FOR J%=SC% TO SC%+1%
2440    FD(J%,1%)=MN(J%)
2450    FD(J%,2%)=MX(J%)
2455    PRINT ,J%,MN(J%),MX(J%)       ! KILL THIS
2460 NEXT J%
2470    FD(9%,0%)=A5(NB%,NC%)
2480    FD(9%,1%)=A5(NB%,NC%)/Nb%    ! THIS MAY BE ADJUSTED.
2490    FD(9%,2%)=NB%
2520 FF$(0%)=B5$(2%)
2530 FF$(1%)=B5$(3%)
2540 PRINT CPOS(8%,5%);'ENTER TWO LINES OF INFORMATION DETAILING LIMITS.'
2550    PRINT CPOS(9%,10%); \ INPUT FF$(1%)
2560    PRINT CPOS(10%,10%); \ INPUT FF$(2%)
2570 PRINT CPOS(7%,1%);ES$+'2K';
2580 PRINT CPOS(7%,5%); 'LIMITS FILE ';FR$;' IS COMPLETE.'
2585 PRINT CPOS(8%,5%);ES$+'J';
2590 CLOSE 5
2600 RETURN
2o10 END
4000! SUBROUTINE NORMAL....RATE SCALING LIMITS DATA NORMALIZATION.
4010!     SCALES AND NORMALIZES EACH DATA CHANNEL TO UNITY USING MAX AND
4020!          MIN DATA STORED IN FR$='Raterun filename.MXM'.
```

```
4060! OPEN DATA FILES. LIMITS FILE #6 ALREADY OPEN.
4070!
4080 OPEN FI$ AS OLD DIM FILE 1                          ! INPUT FILE.
4090     DIM #1,BI$(6)=64%,A1(VAL(BI$(1)),VAL(BI$(0)))
4093     NC%=VAL(BI$(0))
4095     NB%=VAL(BI$(1))
4100 OPEN FO$ AS NEW DIM FILE 2 SIZE 2*NB%/64%+2%       ! OUTPUT FILE.
4110     DIM #2,B2$(6%)=64%,A2(VAL(BI$(1)),1%)
4120!
4130! FILTER INITIALIZATION
4140!
4200 DIM AF(NB%,2%)
4210 FOR J%=1% TO 2%
4220    SF(J%)=(FD(J%,2%)-FD(J%,1%))      ! SCALE FACTOR CALCULATION.
4240    MN(J%)=FD(J%,1%)                    ! MINIMUM FOR EACH CHANNEL.
4250 NEXT J%
4260!
4270! FILTER AND NORMALIZATION PROCESSING LOOP.
4280!
4290 FOR I%=0% TO NB%-1%
4330       AF(I%,0%)=(A1(I%,SC%)-MN(1%))/SF(1%)-.5          ! SCALE DOWN.
4332       AF(I%,1%)=(A1(I%,SC%+1%)-MN(2%))/SF(2%)-.5         ! SCALE DOWN.
4345 NEXT I%
4350 FOR I%=0% TO NB%-1%
4353    IF SC%=1% THEN A2(I%,0%)=A1(I%,0%)  \  GOTO 4380 ! RATE DATA ON LINE 0
4355    A2(I%,0%)=A1(I%,NC%)
4380    A2(I%,1%)=AF(I%,1%)-AF(I%,0%)
4395 NEXT I%
4401!
4403 B2$(0%)=NUM$(1%)
4404 B2$(1%)=BI$(1%)
4405 B2$(2%)=FO$
4406 B2$(1%)=BI$(1%)
4407 FOR J%=3% TO 6%
4408 B2$(J%)=BI$(J%)
4409 NEXT J%
4410!
4450 CLOSE 1,2,5,6
4460 RETURN
4470!
```

HPLOT1

HPLOT1 is a general-purpose plot routine that drives an Hp 7225A plotter. The input data format is the same as the output of DATRUN. The operator has control over the axis scaling, titles, and which data to plot. The routine is capable of plotting up to 4 channels of data on a single graph.

```
10 ! 'HPLOT1'.... ROUTINE TO DO MULTIPLE PLOTS ON HP 7225A
11 !  JOEL HANSE 6/10/80
12 !
13 ! PLOTTER IS CONNECTED  IEEE-488 PORT '105'
15 ! DATA IS ASSUMED TO BE A DATRUN FORMAT VIRTUAL ARRAY
17 !
18 ES$=CHR$(27)+"["
19 PRINT ES$+"2J";CPOS(3,1)
20 ON CTRL/C GOTO 1240
30 ON ERROR  GOTO 1240
32 INIT PORT 1
35 PRINT 'HPLOT1....HP 7225A PLOTTING ROUTINE FOR DATRUN FORMAT FILES.'
37 PRINT
40 PRINT 'ENTER FILE NAME';\ INPUT FI$
50 PC%=1                ! PLOT COUNTER FOR MULTIPLE PLOTS
60 PRINT FI$;' IS ASSUMED TO BE A DATRUN VIRTUAL ARRAY FILE.'
65 PRINT 'ENTER PLOT HEADING'; \ INPUT PH$
70 DIM X(500),Y(500)
80 OPEN FI$ AS OLD DIM FILE 1
90 DIM #1,B2$(6)=64%,V(VAL(B2$(1)),VAL(B2$(0)))
100 IF PC%<>1 GOTO 140
110 PRINT 'ENTER COLUMN  FOR X AXIS';\INPUT IX%
120 PRINT 'IS X AXIS THE TACH OUTPUT';\INPUT KR$
130 IF LEFT(KR$,1)='Y' THEN KR=60/1.10 ELSE KR=1
140 PRINT 'ENTER COLUMN  FOR Y AXIS';\INPUT IY%
150 NC%=VAL(B2$(0))
160 IF IY%<0 THEN 1240
170 IF IX%>NC% OR IY%>NC% THEN 100
172 IF PC%<>1 GOTO 240
180 NP%=VAL(B2$(1))
190 PRINT 'DATA POINTS IN FILE=';NP%
200 PRINT 'ENTER # OF DATA POINTS TO PLOT';\INPUT NP%
210 !                   READ IN THE X AND Y AXIS AND COMPUTE MAX AND MIN VALUES
230 XX=-1E30\XM=1E30
240 YY=-1E30\YM=1E30
241 V(NP%,IY%)=V(NP%-1%,IY%)
250 FOR J%= 1 TO NP%-1%
260    IF PC% <> 1% GOTO 300
270    X(J%)=V(J%,IX%)*KR
280    IF X(J%)>XX THEN XX=X(J%)
290    IF X(J%)<XM THEN XM=X(J%)
300    D3=ABS(V(J%+1%,IY%)-V(J%-1%,IY%))     ! WILD POINT EDITOR
302    D2=ABS(V(J%+1%,IY%)-V(J%,IY%))
304    D1=ABS(V(J%,IY%)-V(J%-1%,IY%))
306    IF D1>50*D3 AND D2>50*D3 THEN Y(J%)=V(J%-1%,IY%) ELSE Y(J%)=V(J%,IY%)
310    IF Y(J%)>YY THEN YY=Y(J%)
320    IF Y(J%)<YM THEN YM=Y(J%)
330 NEXT J%
335    Y(0%)=V(0%,IY%)\X(0%)=V(0%,IX%)*KR
340    IF PC%<>1 GOTO 370
350    PRINT 'X MAX AND MIN VALUES ARE';XX,XM
360    PRINT 'ENTER X AXIS MAX AND MIN FOR THE PLOT';\INPUT SS,SM
361    IF SS>SM THEN XX=SS ELSE XX=SM
362    IF SS>SM THEN XM=SM ELSE XM=SS
370    PRINT 'Y MAX AND MIN VALUES ARE';YY,YM
```

```
380     PRINT 'ENTER Y AXIS MAX AND MIN FOR THE PLOT'\INPUT SS,SM
381     IF SS>SM THEN YY=SS ELSE YY=SM
382     IF SS>SM THEN YM=SM ELSE YM=SS
390     IF PC%<>1% GOTO 420
400     XL=6.\YL=6.
410 PRINT 'ENTER X AXIS LABEL'\INPUT LX$
420 PRINT 'ENTER Y AXIS LABEL'\INPUT LY$
430 !                          CALCULATE THE RESOLUTION FOR THE PLOT
440 ! RX IS THE RESOLUTION FOR THE X AXIS
450 ! RY IS THE RESOLUTION FOR THE Y AXIS
460 RS=10000
470 IF ABS(XX)>ABS(XM) THEN RX=ABS(XX) ELSE RX=ABS(XM)
480 RX=RS/RX
490 IF ABS(YY)>ABS(YM) THEN RY=ABS(YY) ELSE RY=ABS(YM)
500 RY=RS/RY
520 !              START PLOTTING
530 O%=105%                                    ! OUTPUT AND INPUT IEEE ADDRESS
540 I%=105%
550 IF PC%= 1% GOTO 600
555 PRINT CHR$(7%);'PEN CHANGE? (Press screen to continue)'\WAIT FOR KEY
556 K%=KEY
570 !
600 PRINT @O%,'IN;SI;'                        ! INITIALIZE PLOTTER
710 !
720 !              SET LIMITS OF THE PLOT
730 PX=1000*(XL+2)\PY=1000*(YL+.5)            ! CALCULATE PLOTTER LIMITS
740 PRINT @O%,'IP 2000,500,';PX;',';PY;';'    ! SEND PLOTTER LIMITS
745 IF PC%<> 1% GOTO 900                      !  SKIP X AXIS FOR MULTI-PLOT
760 ! PUT ON X AXIS
770 PRINT @O%,'PA2000,500;PD;XT;'
780 FOR I=1 TO XL
790 PRINT @O%,'PR1000,0;XT;'
800 NEXT I
810 PRINT @O%,'PU;'
820 PRINT @O%,'PA4000,100;LB';LX$;CHR$(3);'';'    ! WRITE LABEL ON X AXIS
830 DX=(XX-XM)/XL
840 PRINT @O%,'PA1400,300;'
850 FOR I=0 TO XL                             ! SCALE NUMBERS
860 Z=XM+DX*I
861 Z$=NUM$(Z,'S####.##')
870 PRINT @O%,'LB';Z$;CHR$(3);'';';'PR118,0;'
880 NEXT I
890 ! END OF X AXIS NOW PUT ON Y AXIS
900 XV%=2500%-PC%*500%
902 PRINT @O%,'PA',XV%,',500;PD;YT;'
910 FOR I=1 TO YL
920 PRINT @O%,'PR0,1000;YT;'
930 NEXT I
940 PRINT @O%,'PU;DIO,1;PR-300,',-YL*750,';LB';IY%;'= ';LY$;CHR$(3);';'
950 DY=(YY-YM)/YL
960 PRINT @O%,'PA',(XV%-150%),',50;'
970 FOR I=0 TO YL
980 Z=YM+DY*I
981 Z$=NUM$(Z,'S###.###')
990 PRINT @O%,'LB';Z$;CHR$(3);';PR0,100;'
```

```
1000 NEXT I
1020 ! END OF Y AXIS
1022 IF PC%<>1 GOTO 1090
1030 ! WRITE LABEL ON AXIS
1040 FOR IL=2 TO 4
1050 PL=PY+1000-(IL-2)*250
1060 PRINT @0%,'PU;DI1,0;PA2000,';PL;';LB';B2$(IL);CHR$(3);';'
1070 NEXT IL
1071 PL=PY+250
1072 PRINT @0%,'PU;DI1,0;PA2000,';PL;';LB';PH$;CHR$(3);';'      ! PLOT HEADER
1090 XM%=INT(XM*RX)\XX%=INT(XX*RX)
1092 YM%=INT(YM*RY)\YY%=INT(YY*RY)
1095 PRINT @0%,'SC';XM%;',';XX%;',';YM%;',';YY%;';'! SCALE PLOT
1100 ! PLOT THE DATA
1124 I=0
1125 PRINT @0%,'PA';INT(X(I)*RX);',';INT(Y(I)*RY);';PD'
1128 FOR I=1% TO NP%-1%
1130 PRINT @0%,'PA';INT(X(I)*RX);',';INT(Y(I)*RY);';PD'
1140! IF I <> 1 THEN PRINT @0%,X(I)*RX;',';Y(I)*RY
1150! IF I<>1 AND I<NP% THEN PRINT @0%,',',
1180 NEXT I
1190 PRINT CHR$(27);'[10D';CHR$(27);'[1K';
1200 PRINT @0%,';PU;PR100,0;DI1,0;LB';IY%;CHR$(3);';IN;'
1210 PC%=PC%+1%\PRINT 'PLOT DONE; NEXT CHANNEL'
1220 PRINT @0%,'PU;'
1230 GOTO 100
1240 PRINT @0%,'IN;'
1260 CLOSE 1
1270 IF ERR <> 0 THEN PRINT 'ERR=';ERR,'ERL=';ERL
1280 END
```